Biogeosciences, 7, 4083–4103, 2010
www.biogeosciences.net/7/4083/2010/
doi:10.5194/bg-7-4083-2010


Biogeosciences

# Fluorescence and absorption properties of chromophoric dissolved organic matter (CDOM) in coastal surface waters of the northwestern Mediterranean Sea, influence of the Rhône River

**J. Para[1,2], P. G. Coble[3], B. Charrière[1,2], M. Tedetti[1,2], C. Fontana[4,5], and R. Sempéré[1]**

[1]Université de la Méditerranée, LMGEM, Centre d'Océanologie de Marseille, Case 901, 13288 Marseille Cedex 9, France
[2]CNRS/INSU, UMR 6117, LMGEM, Case 901, 13288 Marseille Cedex 9, France
[3]College of Marine Science, University of South Florida, 140 7th Avenue, St. Petersburg, Florida 33701, USA
[4]Université de la Méditerranée, LOPB, Centre d'Océanologie de Marseille, UMR 6535, Station Marine d'Endoume, Chemin Batterie des Lions, 13007 Marseille, France
[5]CNRS/INSU, UMR 6535, LOPB, Centre d'Océanologie de Marseille, Station Marine d'Endoume, Chemin Batterie des Lions, 13007 Marseille, France

Received: 28 June 2010 – Published in Biogeosciences Discuss.: 22 July 2010
Revised: 7 December 2010 – Accepted: 17 December 2010 – Published: 23 December 2010

**Abstract.** Seawater samples were collected monthly in surface waters (2 and 5 m depths) of the Bay of Marseilles (northwestern Mediterranean Sea; 5°17′30″ E, 43°14′30″ N) during one year from November 2007 to December 2008 and studied for total organic carbon (TOC) as well as chromophoric dissolved organic matter (CDOM) optical properties (absorbance and fluorescence). The annual mean value of surface CDOM absorption coefficient at 350 nm [$a_{CDOM}(350)$] was very low ($0.10 \pm 0.02\,m^{-1}$) in comparison to values usually found in coastal waters, and no significant seasonal trend in $a_{CDOM}(350)$ could be determined. By contrast, the spectral slope of CDOM absorption ($S_{CDOM}$) was significantly higher ($0.023 \pm 0.003\,nm^{-1}$) in summer than in fall and winter periods ($0.017 \pm 0.002\,nm^{-1}$), reflecting either CDOM photobleaching or production in surface waters during stratified sunny periods. The CDOM fluorescence, assessed through excitation emission matrices (EEMs), was dominated by protein-like component (peak T; 1.30–21.94 QSU) and marine humic-like component (peak M; 0.55–5.82 QSU), while terrestrial humic-like fluorescence (peak C; 0.34–2.99 QSU) remained very low. This reflected a dominance of relatively fresh material from biological origin within the CDOM fluorescent pool. At the end of summer, surface CDOM fluorescence was very low and strongly blue shifted, reinforcing the hypothesis of CDOM photobleaching. Our results suggested that unusual Rhône River plume eastward intrusion events might reach Marseilles Bay within 2–3 days and induce local phytoplankton blooms and subsequent fluorescent CDOM production (peaks M and T) without adding terrestrial fluorescence signatures (peaks C and A). Besides Rhône River plumes, mixing events of the entire water column injected relative aged (peaks C and M) CDOM from the bottom into the surface and thus appeared also as an important source of CDOM in surface waters of the Marseilles Bay. Therefore, the assessment of CDOM optical properties, within the hydrological context, pointed out several biotic (in situ biological production, biological production within Rhône River plumes) and abiotic (photobleaching, mixing) factors controlling CDOM transport, production and removal in this highly urbanized coastal area.

*Correspondence to:* R. Sempéré
(sempere@univmed.fr)

## 1 Introduction

Dissolved organic matter (DOM) represents one of the largest bioreactive organic reservoirs at earth's surface (Hedges, 1992, 2002) and constitutes the main substrate for heterotrophic bacteria growth (Azam et al., 1983). The dominant source of DOM in the ocean is phytoplankton through release of organic compounds during bacterial and viral lysis, exudation, excretion and grazing (Mague et al., 1980; Jumars et al., 1989; Nagata, 2000; Myklestad, 2000). Though the inputs of terrestrial DOM represent only 0.7–2.4% of the total oceanic DOM pool, river inputs may be important in coastal oceanic areas (Opsahl and Benner, 1997) by

fueling alternative labile carbon source to sustain local carbon demand in addition to autochthonous carbon source derived from phytoplankton and heterotrophic microbial food web (Sempéré et al., 2000) and increasing light attenuation (Blough and Del Vecchio, 2002; Nelson and Siegel, 2002).

Chromophoric (or colored) dissolved organic matter (CDOM), which is the fraction of DOM that absorbs light over a broad range of ultraviolet (UV) and visible wavelengths, is essentially controlled by in situ biological production, terrestrial inputs (sources), photochemical degradation, microbial consumption (sinks), as well as deep ocean circulation (Siegel et al., 2002; Nelson et al., 2007; Coble, 2007) and upwelling and/or vertical mixing (Coble, 1996; Parlanti et al., 2000). CDOM is the major factor controlling the attenuation of UV radiation in the ocean (Kirk, 1994) and is highly photoreactive and efficiently destroyed upon exposure to solar radiation (Mopper and Kieber, 2000, 2002).

In the past 20 years, CDOM fluorescence properties have been widely studied owing to excitation-emission matrices (EEMs). Coble et al. (1990) highlighted that the fluorescence properties of the Black Sea CDOM came from two types of fluorescent peaks (humic-like and protein-like). Protein-like fluorescence, considered as a proxy for labile DOM (Yamashita and Tanoue, 2003), has been frequently reported (Mopper and Schultz, 1993; De Souza-Sierra et al., 1994; Determann et al., 1994, 1996; Coble, 1996; Mayer et al., 1999). The identification/quantification of humic-like and protein-like peaks from EEMs has thus allowed determining the dynamics of DOM in relation to its biological reactivity. In addition, fluorescence indices have also been used to assess the origin and dynamics of fluorescent CDOM, especially in the coastal areas subjected to freshwater inputs. The humification index (HIX, Zsolnay et al., 1999) and the biological index (BIX, Huguet et al., 2009) have been employed to determine the relative degree of humification and autotrophic productivity of fluorescent CDOM, respectively.

Freshwater inputs play a major role in the biogeochemistry of the coastal areas with a world annual fresh water discharge of 40 000 $km^3$, more than 25 billions tons of particulate and dissolved matter (Milliman et al., 1995) and transporting on average $1 \pm 0.2$ Gt of carbon per year in particulate and dissolved forms (Amiotte-Suchet et al., 2003). In the Mediterranean Sea, freshwater inputs enhance significantly primary productivity (Cruzado and Velasquez, 1990; Joux et al., 2009). The annual fluvial loading of TOC to the Mediterranean Sea comprises 0.08–0.3% of the standing stock of TOC in the whole Mediterranean Basin (Sempéré et al., 2000), which is much higher than the average value reported for the World Ocean (0.024%, Smith and Hollibaugh, 1993). Since the damming of the Nile, the Rhône River became the major source of fresh water and terrigenous particles to the Mediterranean basin (Margat, 1992). Its mean freshwater discharge is around 1700 $m^3 s^{-1}$, which represents 90% of the total freshwater input in the Gulf of Lion's continental shelf (Durrieu de Madron et al., 2003) and ∼3–14% and 10–12% of the overall total organic and inorganic carbon (TOC and TIC) river inputs to the Mediterranean Sea (Sempéré et al., 2000). Remote sensing observations (Forget et al., 1990; Devenon et al., 1992; Broche et al., 1998) and modeling studies (Estournel et al., 2001; Arnoux-Chiavassa et al., 2003; Reffray et al., 2004) shown the predominant westward direction of the Rhône River plume with an extent and a thickness depending on its discharge, the meteorological conditions and the surrounding circulation, particularly the Northern Current. A less common orientation of the Rhône River plume, towards the east as far as 40 km from the Rhône River mouth and offshore of Marseilles Bay, has been recently documented by using the acoustic Doppler current profiler (ADCP) measurements (Gatti et al., 2006).

Despite its relative significant role in the Mediterranean carbon cycle, there are only a few studies showing CDOM originating either directly from the Rhône River or from by-products of primary production in coastal areas or more generally in the northwestern Mediterranean Sea (Ferrari et al., 2000; Babin et al., 2003; Vignudelli et al., 2004). Moreover, with an annual average of total solar radiation of 162 $W m^{-2}$ (Ruiz et al., 2008), the western Mediterranean basin is characterized by relatively high solar radiation levels due to its weak cloud cover (Vasilkov et al., 2001; Seckmeyer et al., 2008; Cristofanelli and Bonasoni, 2009; The MERMEX Group, 2010). High surface irradiances coupled to a strong penetration of UV and visible radiation (Tedetti and Sempéré, 2006 and references therein; Joux et al., 2009) could impact the CDOM content as well as primary productivity in the surface waters of the Mediterranean Sea.

Here we report CDOM absorbance and fluorescence data from a one-year time series in the Bay of Marseilles. This study aims to better understand coastal surface CDOM distribution and dynamics of the Mediterranean Sea. Origins as well as seasonal variation of CDOM are discussed considering the potential influence of Rhône River plume.

## 2 Materials and methods

### 2.1 Study site and sample collection

From November 2007 to December 2008, surface seawater samples (2 and 5 m depths) were collected monthly close to solar noon on board the R/V *Antedon II* at the observation station of the Oceanology Center of Marseilles: SOFCOM. This coastal station is located 5 km off Marseilles in the northwestern Mediterranean Sea (Fig. 1) and is one of the French Service d'Observation en Milieu LITtoral (SOMLIT, http://www.domino.u-bordeaux.fr/somlit_national/) coastal stations, which have been regularly sampled (twice a month) for 13 years. Samples were collected using Niskin bottles equipped with Teflon-O-ring and silicon tubes. Surface irradiance ($E_s(\lambda)$ in $\mu W cm^{-2}$) measurements in the UV (305, 325, 340, 380 nm) spectral

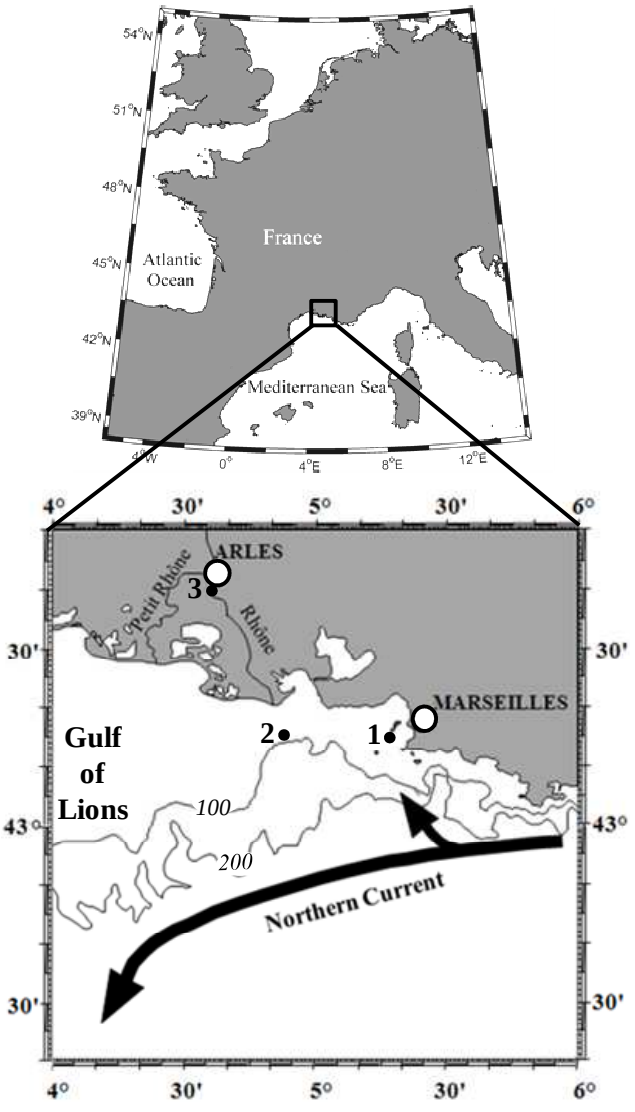


**Fig. 1.** Map of the Bay of Marseilles marking the location of SOFCOM station (black dot 1) in the Bay of Marseilles, the two Rhône Estuary stations (black dot 2) and Arles station (black dot 3). Distance separating SOFCOM station from Rhône River Estuary is around 40 Km.

domain were also performed using OCR-504 downward irradiance sensors on the ship's deck. During this study period, water samples were also collected at 2 m depth in the Rhône River at Arles station, and from 2 and 5 m depths at two stations in the Rhône River Estuary during the CHACCRA-plume cruise (May 2008) (Fig. 1).

For TOC determination, samples were directly transferred from the Niskin bottle into precombusted (6 h at 450 °C) ampoules, immediately acidified with 85% of $H_3PO_4$ (final pH∼2) and flame sealed without filtration. For the determination of CDOM optical properties (absorbance and fluorescence), samples were transferred from Niskin bottles into 10% HCl washed and precombusted (6 h at 450 °C) glass bottles and stored in the dark. Samples were brought back to the laboratory, filtered in dim light through precombusted 0.7 µm GF/F filters, which had been pre-rinsed with Milli-Q water and sample, and then through 0.2 µm Nuclepore polycarbonate filters, presoaked in 10% HCl solution and rinsed with Milli-Q water and with sample according to the SeaWiFS protocols (Mueller and Austin, 1995). Filtered samples were kept in the dark at room temperature (24 h maximum) until absorbance and fluorescence analyses. During the study period, in situ hydrological context was determined at least twice a month by the Service d'Observation of the Oceanology Center of Marseilles by using a SeaBird Electronics 19 *plus* conductivity temperature depth (CTD) profiler. In addition, from February 2008 onwards, the hydrological data set was completed with a SeaBird Electronics 19 *plus* CTD equipped with chlorophyll-*a* (Chl-*a*) fluorometer (WET Labs Inc.) deployed during our sampling.

### 2.2 CDOM optical properties

#### 2.2.1 Absorbance measurements

Absorbance of CDOM was measured throughout the UV and visible spectral domains (280–700 nm) using the multiple pathlength, liquid core waveguide system Ultrapath (MPLCW, WPI Inc.). Absorbance spectra of marine and freshwater samples were measured through 2 m and 50 cm long pathlengths, respectively. Marseilles' Bay (SOFCOM station) and Rhône plume (marine) samples were analysed with reference to a filtered salt solution prepared with Milli-Q water and precombusted NaCl (Sigma) reproducing the refractive index of samples to minimize baseline offsets in absorption spectra induced by the effect of salinity changes between sample and the corresponding reference (D'Sa et al., 1999). Rhône River (freshwater) samples were analyzed with reference to filtered Milli-Q water. Reference salt solution and samples were brought to room temperature before analysis. Between each sample, the sample cell was flushed with successively diluted detergent (cleaning solution concentrate, WPI Inc.), high reagent grade MeOH, 2 M HCl and Milli-Q water. Cleanliness of the sample cell was checked by comparing with a reference value for the transmittance of the reference salt solution. Trapped microbubbles were minimized by using a peristaltic pump to draw the sample into the sample cell. The spectral absorption coefficients, $a_{\mathrm{CDOM}}(\lambda)$ ($\mathrm{m}^{-1}$) were obtained using the following relationship, $a_{\mathrm{CDOM}}(\lambda) = 2.303\, A(\lambda)/L$, where $A(\lambda)$ is the absorbance at wavelength $\lambda$ (dimensionless) and $L$ is the pathlength in meters. All samples that had an absorbance value above 0.2 at 300 nm for a 10 cm cell were corrected for the inner filter effect according to the formula proposed by Ohno (2002). Value of spectral slope of CDOM absorption ($S_{\mathrm{CDOM}}$) has most often been determined using an exponential regression (Jerlov, 1968; Bricaud et al., 1981)

but non-linear regression fitting provides a better estimate of $S_{CDOM}$, by weighting regions of higher CDOM absorption (Stedmon et al., 2000). Here, $S_{CDOM}$ was determined after applying a non-linear exponential regression to original $a_{CDOM}(\lambda)$ data measured on the range 350–500 nm. All the determination coefficients ($R^2$) calculated from these exponential fits were always >0.99. $S_{CDOM}$ provides information concerning CDOM origin (terrestrial versus marine), with generally lower slopes in fresh and coastal waters than in the open ocean due to the presence of marine humics and new biological CDOM (Ferrari et al., 2000; Blough and Del Vecchio, 2002). Additionally, higher $S_{CDOM}$ have been reported for photobleached CDOM (Vodacek et al., 1997).

#### 2.2.2 Fluorescence measurements

For fluorescence measurements, performed monthly, from June 2008 to December 2008, samples were transferred into a 1 cm pathlength far UV silica quartz cuvette (170–2600 nm; LEADER LAB), thermostated at 20 °C, and analyzed with a Hitachi (Japan) Model F-7000 spectrofluorometer. Instrument settings, measurement procedures and spectral correction procedures are fully described in Tedetti et al. (2010). Briefly, the correction of spectra for instrumental response was conducted according to the procedure recommended by Hitachi (Hitachi F-7000 Instruction Manual). First, the Ex instrumental response was obtained by using Rhodamine B as standard and a single-side frosted red filter in Ex scan mode. Then, the Em side calibration was done with a diffuser in synchronous scan mode. The Ex and Em spectra obtained over the range 200–600 nm were applied internally by the instrument to correct subsequent spectra. EEMs were generated over Ex wavelengths between 200 and 550 nm in 5 nm intervals and Em wavelengths between 280 and 600 nm in 2 nm intervals, with 5 nm bandwidths (FWHMs) on both Ex and Em sides and a scan speed of 2400 nm min$^{-1}$. Milli-Q water as well as solutions of quinine sulphate (Fluka) in 0.05 M $H_2SO_4$ (1–10 ppb) were run with each set of samples. Before being processed, all the data (blanks, standards, samples) were normalized to the intensity of the Raman scatter peak at Ex/Em: 275/303 nm (5 nm bandwidths) of pure water (Coble et al., 1993; Coble, 1996; Belzile et al., 2006), which varied by less than 4% over the study period. Samples were then corrected for the corresponding blanks and converted into quinine sulphate units (QSU). EEM data processing and contour plots were conducted with MATLAB 7.1.

Besides the identification of common fluorescent peaks by the traditional "peak picking" technique (examination of Ex and Em spectra), we determined two indices: the humification index (HIX) and the biological index (BIX). HIX was introduced on the basis of the position of the emission spectra in order to estimate the degree of maturation of DOM in soil (Zsolnay et al., 1999). It is the ratio ($H/L$) of two areas of emission spectrum from excitation at 254 nm (here 255 nm). These two areas are calculated between 300 and 345 nm (here, between 300–346 nm) for $L$ and between 435 and 480 nm (here, between 434–480 nm) for $H$. In natural aquatic ecosystem (Gironde and Seine estuaries and Mediterranean Sea), high values of HIX (10–16) illustrated the presence of strongly humic organic material (terrestrial origin), whereas low values (<4) represent authochtonous organic material (Huguet et al., 2009). BIX allows the determination of the presence of the marine humic-like peak (peak M), which reflects autochthonous biological activity (Huguet et al., 2009). It is calculated at Ex = 310 nm, by dividing the fluorescence intensity at Em = 380 nm (maximum of M peak) by the fluorescence intensity at Em = 430 nm, which corresponds to the maximum of peak C. High values of BIX (>1) correspond to a biological origin and lowest values (<1) illustrate low abundance of organic matter of biological origin (Huguet et al., 2009). Analytical errors of these indices were within 5%.

### 2.3 TOC analysis

The Shimadzu instrument used in this study is the commercially available model TOC-5000 Total Carbon Analyzer with a quartz combustion column filled with 1.2% Pt on silica pillows. Several aspects of our modified unit have been previously described (Sohrin and Sempéré, 2005). The accuracy and the system blank of our instrument were determined by the analysis of the reference material (D. Hansell, Rosenstiel School of Marine and Atmospheric Science, Miami, USA) including Deep Atlantic Water (DAW) and low carbon water (LCW) reference standards. The average DOC concentrations in the DAW and in the LCW reference standards were $45 \pm 2$ µM C, $n = 24$ and $1 \pm 0.3$ µM C, $n = 24$, respectively. Carbon levels in the LCW ampoules were similar to and often higher than the Milli-Q water produced in our laboratory. The nominal analytical precision of the analysis procedure was within 2%.

### 2.4 Remotely sensed data

Remotely sensed images of SST and Chl-*a* concentration (Fig. 2) were obtained by applying respectively the long-wave SST algorithm and the OC5 coastal-oriented optical algorithm (Gohin et al., 2002, 2005) to water leaving irradiances derived from the Moderate Resolution Imaging Spectroradiometer (MODIS) sensor. Accuracy of the OC5 algorithm applied to the Rhône River plume region has been estimated to be 40% absolute percentage of difference by comparing 332 in situ and co-localized remotely sensed values of Chl-*a* concentrations using the Sea-viewing Wide Field of View Sensor (SeaWiFS) (Fontana et al., 2009).

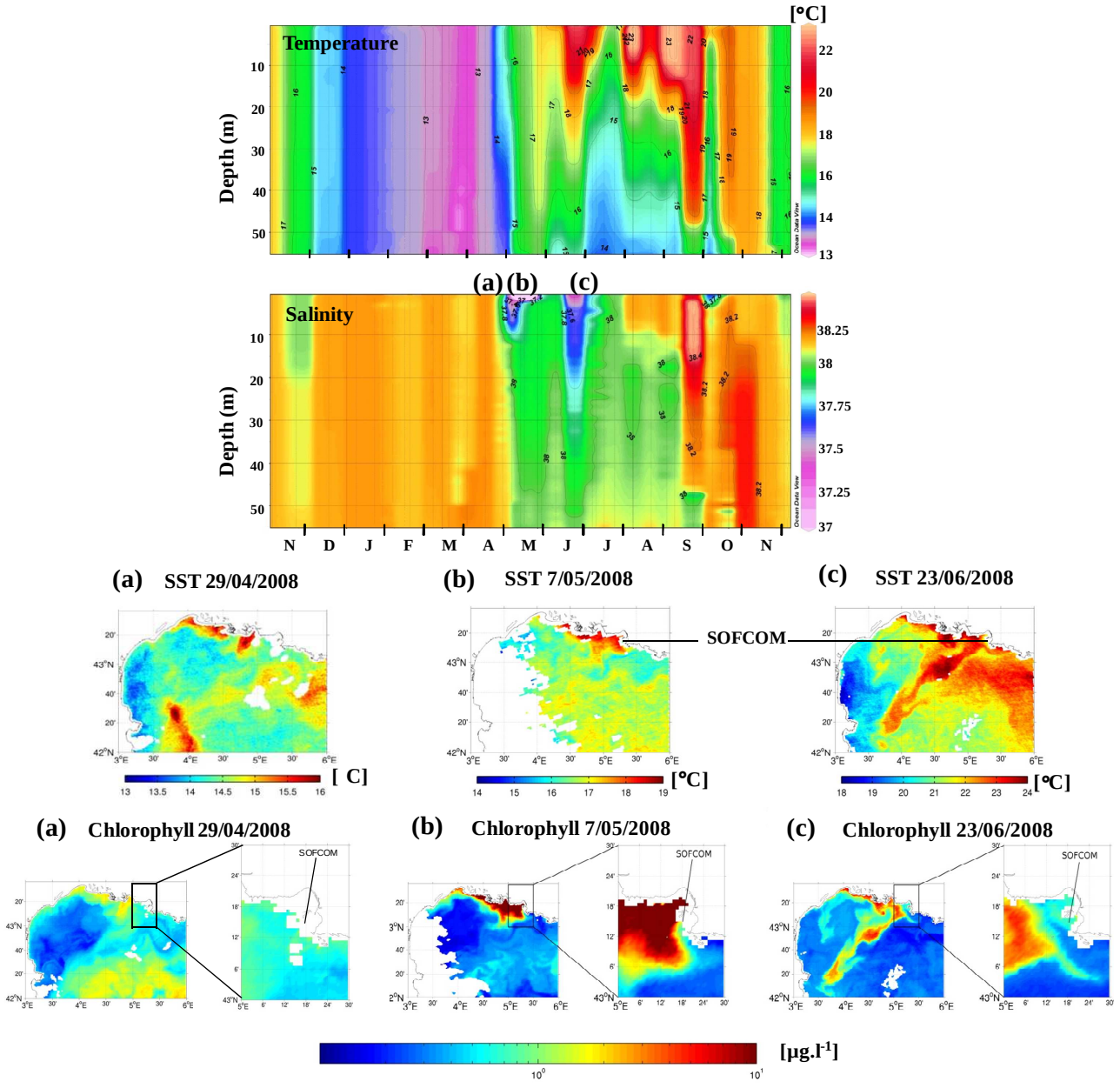


**Fig. 2.** Top panels: temporal evolution of temperature and salinity at SOFCOM station from November 2007 to December 2008 from surface to bottom. Data come from CTD profiles carried out twice a month by the SOMLIT network ($n = 30$) and completed since February 2008 by CTD data acquired on sampling dates ($n = 11$). Bottom panels: remotely sea surface temperature (SST) and chlorophyll concentrations are from the points in the time series labeled **(a)**, **(b)** and **(c)** corresponding respectively to the sampling date 29 April (non-intrusion of Rhône plume), 7 May and 23 June 2008 (intrusion of Rhône plume). Remotely SST and Chlorophyll concentrations from satellite images were obtained respectively by applying the long-wave SST algorithm and the OC5 coastal-oriented optical algorithm (Gohin et al., 2002, 2005) to water leaving irradiances derived from the Moderate Resolution Imaging Spectroradiometer (MODIS).

### 2.5 Irradiation experiment on Rhône River water

A kinetic irradiation experiment was carried out on a Rhône River sample collected at Arles station on 7 February 2009 (2 m depth). The 0.2 µm filtered solution was distributed in 50 ml precombusted (450 °C, 6 h) quartz tubes and placed in thermostated bath at 13 °C. Samples were exposed to a simulated sunlight using a Suntest CPS + solar simulator (Atlas, GmbH) in Full Sun (FS) light condition (i.e., FS = PAR + UVB + UVA) giving an optical output of 700 W m$^{-2}$. Exposure for 2.8 h at this intensity corresponds to a natural daily (12 h) dose received in the Western

Mediterranean Basin by taking an annual average of total solar radiation of 162 W m$^{-2}$ (Ruiz et al., 2008). Samples were irradiated in duplicate during 8 (T1) and 20 h (T2) which corresponds to 3 and 7 days of natural solar irradiation, respectively. Simultaneous dark control (quartz tube wrapped in black bag) was performed under the same conditions.

## 3 Results

### 3.1 Hydrological context and trophic status

During winter and fall periods, the action of winds mixed entirely the water column of Marseilles Bay (60 m depth). The general trend observed from the surface to the bottom during this stormy period was a salinity around 38.1–38.2 and a temperature decreasing from 18 to 15 °C in fall and from 15 to 13 °C in winter (Fig. 2). These are the typical values recorded for the northwestern Mediterranean Sea (Brasseur et al., 1996). At the beginning of spring, the entire water column was still well mixed and exhibited a temperature and a salinity corresponding to those observed during winter (Fig. 2). During May, water began warming (16–17 °C) causing the formation of a thermocline around 40 m depth. Early in May, an intrusion of a less salty water mass (37–37.8) was observed in the upper 10 m. The low salinity surface water mass, perhaps coupled with physical forcing, seems to have also impacted the salinity signature of the deepest water because the salinity of the latter was <38 down to 45 m, whereas the salinity value of deeper Mediterranean water masses are usually close to 38.3 (Brasseur et al., 1996). At the end of June, another important surface intrusion of low salinity water occurred with a salinity ranging from 37.3 to 37.8 and a temperature ranging from 21.5 to 18 °C between 1 and 30 m depth, respectively. As for the previous low salinity intrusion, this one also appeared to influence the salinity signature of deeper water masses.

These two surface intrusions of low salinity water were also identified by remotely sensed pictures of SST and Chl-*a* concentration on 7 May 2008 (nearest date available corresponding to the sampling date 6 May 2008) on 23 June 2008 (sampling date) and were shown on Fig. 2 (insets b and c). These remotely sensed pictures plus those available encompassing sampling dates (not shown) illustrate clearly that surface inputs of freshwater observed on 6 May 2008 and on 23 June 2008 in Bay of Marseilles came from the eastward extent of the Rhône River plume. In order to have an estimate of the spreading time of the Rhône River plume, successive satellite pictures were used to track the plume. Using the ones encompassing the Rhône River plume intrusion observed on 6 May 2008, we estimated the spreading time to be on the order of 2–3 days, which is in good agreement with the time scale determined by Fontana et al. (2010).

In July, 3 consecutive days of wind from north (Mistral wind) mixed the water column, removing all signs of the Rhône River plume and resulting in a cooling (14–15 °C) coupled to an increase of salinity (38.1) of surface waters (Fig. 2). Sea surface temperature dropped to 16.5 °C at 1 m depth, which is a specific feature of the Bay of Marseilles during stratification period under Mistral wind influence. The last part of summer (August) was more common with the re-establishment of the thermocline around 15–20 m depths separating warm (18–23 °C) and salty (38.2) surface waters from cold deep waters (14–18 °C) of slightly lower salinity (38). At the end of summer (23 September 2008), a warm (21–22 °C) high salinity (>38.4) water mass was observed from a depth of 20 m to the surface which was replaced on 14 October 2008 by a shallower low salinity water mass (37.6) in the upper 3 m due to intense rains. Other slightly less saline water masses in surface were observed at the end of November 2007 and early in December 2008 but during these windy periods, surface low salinity water masses were attenuated and disappeared rapidly due to the mixing (Fig. 2).

In early May and at the end of June 2008, the influence of the eastward extent of the Rhône River could have increased nitrate concentrations within the plume along a gradient of salinity (10–36) from 90 to 15 µM (Pujo-Pay et al., 2006) as well as others nutrients to lesser extent. Phytoplankton biomass in the Bay of Marseilles was enhanced with a value of Chl-*a* concentration >1µg l$^{-1}$, while without the influence of the Rhône River plume Chl-*a* concentration remained <1µg l$^{-1}$ (Table 1, Fig. 2 insets). In May 2008, surface (2 m depth) DOC values decrease from 113±12 µM C in the Rhône River to 74–78 µM C in the Rhône Estuary. These latest values are lower than those previously reported in the Rhône Estuary by Ferrari et al. (2000) (140 µM C).

At SOFCOM station (Table 1), TOC concentrations at both depths studied were similar and were also comparable to DOC concentrations previously reported in open waters of Mediterranean Sea (Doval et al., 1999; Dafner et al., 2001; Santinelli et al., 2002; Sempéré et al., 2002; Seritti et al., 2003), with a stable annual mean of 67±7 µM C at 2 m and 63±6 µM C at 5 m. Thus, despite some episodic influence of the Rhône River plume, this coastal area exhibited features including Chl-*a* concentration <1µg l$^{-1}$ and TOC concentration ∼DOC concentration, which is usually encountered offshore. It is important to notice that during the period study, this coastal oligotrophic area is subjected to a strong UV surface irradiance particularly in spring and summer periods for UVB (305 nm) radiation with surface irradiance ($E_s$) values as high as 4.64 µW cm$^{-2}$ nm$^{-1}$ for UVB (305 nm) in summer time (Table 1) around solar noon. With the exception of sampling dates that were cloudy, we observed around 10 fold more UVB (305 nm) and 2–3 fold more UVA (325, 340 and 380 nm) radiation in summer and spring compared to fall and winter periods.

**Table 1.** Absorption coefficient of CDOM at 350 nm [$a_{CDOM}(350)$], spectral slope of CDOM ($S_{CDOM}$), total organic carbon (TOC) concentration, chlorophyll-*a* concentration (Chl-*a*) and mean surface irradiance ($E_s$) in the UVB (305 nm) and UVA (325, 340, 380 nm) spectral domains measured during one hour close to solar noon, determined at SOFCOM and Rhône Estuary stations at 2 and 5 m depths and Arles station (Rhône and Rhône irradiation experiment: Rhône Irrad. Exp.) at 2 m depth.

| | | $a_{CDOM}(350)$ [$m^{-1}$] | | $S_{CDOM}$ [$nm^{-1}$] | | TOC [µMC] | | Chl-*a* [$\mu g\,l^{-1}$] | | $E_s$(UV) [$\mu W\,cm^{-2}\,nm^{-1}$] | | | | $T$ [°C] | | Salinity | |
|---|---|---|---|---|---|---|---|---|---|---|---|---|---|---|---|---|---|
| End-member | Date | 2 m | 5 m | 2 m | 5 m | 2 m | 5 m | 2 m | 5 m | 305 nm | 325 nm | 340 nm | 380 nm | 2 m | 5 m | 2 m | 5 m |
| SOFCOM[a] | 7 Nov 2007 | 0.11 | 0.1 | 0.018 | 0.019 | 68 | 62 | – | – | 0.51 ± 0.03 | 12.78 ± 0.39 | 20.74 ± 0.59 | 29.17 ± 0.73 | 17.8 | 17.8 | 38.1 | 38.1 |
| SOFCOM | 19 Dec 2007 | 0.1 | 0.1 | 0.017 | 0.018 | 60 | 54 | – | – | 0.14 ± 0.01 | 9.94 ± 0.06 | 17.13 ± 0.11 | 26.46 ± 0.11 | 14.4 | 14.4 | 38.2 | 38.2 |
| SOFCOM | 5 Feb 2008 | 0.11 | 0.11 | 0.016 | 0.015 | – | 55 | 0.90 | 0.92 | 0.48 ± 0.01 | 15.72 ± 0.09 | 25.56 ± 0.17 | 36.19 ± 0.38 | 13.2 | 13.2 | 38.1 | 38.1 |
| SOFCOM | 14 Feb 2008 | 0.09 | 0.09 | 0.018 | 0.018 | 78 | 61 | 0.20 | 1.03 | 0.42 ± 0.01 | 16.86 ± 0.08 | 27.90 ± 0.19 | 38.81 ± 0.23 | 13.2 | 13.3 | 38.1 | 38.1 |
| SOFCOM[a] | 26 Mar 2008 | – | 0.1 | – | 0.016 | 56 | 59 | 0.21 | 0.24 | 1.39 ± 0.03 | 25.85 ± 0.34 | 39.09 ± 0.61 | 52.86 ± 0.98 | 12.8 | 12.8 | 38.1 | 38.1 |
| SOFCOM | 29 Apr 2008 | 0.11 | 0.11 | 0.018 | 0.020 | 70 | 63 | 0.85 | 0.89 | 3.09 ± 0.09 | 36.62 ± 1.25 | 54.67 ± 2.29 | 74.18 ± 3.17 | 14.5 | 14.4 | 38.1 | 38.1 |
| SOFCOM[a] | 6 May 2008 | 0.13 | 0.13 | 0.018 | 0.018 | 65 | – | 1.55 | 1.69 | 0.93 ± 0.05 | 12.83 ± 0.72 | 18.81 ± 1.08 | 24.47 ± 1.48 | 16.1 | 16.0 | 37.1 | 37.3 |
| SOFCOM[a] | 9 Jun 2008 | 0.11 | 0.1 | 0.022 | 0.023 | 70 | 61 | 0.77 | 0.86 | 2.26 ± 0.09 | 27.87 ± 1.07 | 40.55 ± 1.65 | 53.69 ± 2.57 | 17.2 | 17.0 | 37.9 | 38.0 |
| SOFCOM | 23 Jun 2008 | 0.12 | 0.11 | 0.026 | 0.026 | 79 | 76 | 1.42 | 1.33 | 4.64 ± 0.06 | 39.14 ± 0.25 | 56.51 ± 0.43 | 77.51 ± 0.81 | 21.4 | 20.8 | 37.5 | 37.5 |
| SOFCOM[b] | 10 Jul 2008 | 0.09 | 0.09 | 0.023 | 0.023 | 67 | 68 | 0.19 | 0.20 | 4.06 ± 0.09 | 40.14 ± 0.92 | 58.88 ± 1.35 | 79.62 ± 1.69 | 18.6 | 17.7 | 37.9 | 37.9 |
| SOFCOM[a] | 23 Sep 2008 | 0.07 | 0.06 | 0.021 | 0.023 | 72 | 67 | 0.40 | 0.45 | 1.13 ± 0.12 | 15.92 ± 1.64 | 23.38 ± 2.62 | 30.98 ± 4.06 | 22.2 | 22.1 | 38.4 | 38.4 |
| SOFCOM[b] | 14 Oct 2008 | 0.09 | 0.09 | 0.018 | 0.018 | 70 | 67 | 0.33 | 0.35 | 1.17 ± 0.01 | 19.58 ± 0.08 | 30.08 ± 0.27 | 43.75 ± 0.51 | 19.4 | 19.4 | 38.2 | 38.2 |
| SOFCOM | 25 Nov 2008 | 0.13 | 0.13 | 0.014 | 0.014 | 55 | 56 | 0.58 | 0.56 | 0.32 ± 0.01 | 13.73 ± 0.01 | 22.88 ± 0.01 | 33.78 ± 0.01 | 15.3 | 15.3 | 38.2 | 38.2 |
| SOFCOM[a] | 4 Dec 2008 | 0.11 | 0.1 | 0.017 | 0.019 | 63 | 65 | 0.76 | 0.96 | 0.18 ± 0.01 | 7.34 ± 0.30 | 11.65 ± 0.48 | 15.28 ± 0.62 | 16.1 | 16.1 | 38.1 | 38.1 |
| Rhône Estuary[c] | 22 May 2008 | 0.25 | 0.09 | 0.019 | 0.021 | 74 | 71 | – | – | – | – | – | – | 16.8 | 17.4 | 33.5 | 37.9 |
| Rhône Estuary[c] | 23 May 2008 | 0.33 | 0.09 | 0.017 | 0.024 | 78 | 67 | – | – | – | – | – | – | 16.7 | 17.6 | 29.9 | 37.7 |
| Rhône (Arles) ($n = 14$)[c] | 17 Jan 2008–18 Nov 2008 | 2.42 ± 1.05 | – | 0.017 ± 0.001 | – | 136 ± 38 | – | – | – | – | – | – | – | – | – | – | – |
| Rhône Irrad. Exp.[c] | T0 | 3.11 | – | 0.018 | – | 163 | – | – | – | – | – | – | – | – | – | – | – |
| Rhône Irrad. Exp.[c] | Dark control | 3.12 | – | 0.018 | – | 157 | – | – | – | – | – | – | – | – | – | – | – |
| Rhône Irrad. Exp.[c] | T1 duplicate | 2.23 ± 0.09 | – | 0.018 ± 0.001 | – | 158 ± 2 | – | – | – | – | – | – | – | – | – | – | – |
| Rhône Irrad. Exp.[c] | T2 duplicate | 1.17 ± 0.05 | – | 0.018 ± 0.000 | – | 150 ± 0 | – | – | – | – | – | – | – | – | – | – | – |

[a] Cloudy day
[b] Sea mist
[c] For Rhône Estuary, Rhône and Rhône Irrad. Exp. end-members, DOC concentration was measured in place of TOC concentration.

### 3.2 CDOM absorbance

The $a_{CDOM}$ at 350 nm was chosen for describing changes in CDOM quantity, and $S_{CDOM}$ to differentiate CDOM quality (Table 1). In the Bay of Marseilles (SOFCOM station), the annual mean values of $a_{CDOM}(350)$ at 2 and 5 m depths were comparable and very low ($0.10 \pm 0.02\,m^{-1}$) with regard to the entire range of the $a_{CDOM}(350)$ found in the literature for diverse aquatic environments (i.e. 0.046–29.9 $m^{-1}$) (Kowalczuck et al., 2003) and thus were more similar to those found offshore. The $a_{CDOM}(350)$ maximum value of $0.13\,m^{-1}$ at 2 and 5 m was observed under Rhône River plume influence (6 May 2008) and during the fall mixing period (25 November 2008), right after 12 consecutive days of Mistral wind that initiated a strong mixing of the entire water column. By contrast, $a_{CDOM}(350)$ minimum value at 2 m ($0.07\,m^{-1}$) and 5 m ($0.06\,m^{-1}$) occurred at the end of summer time (23 September 2008) (Table 1), when the highest salinity (>38.4) and high temperature (22 °C) water was observed (Fig. 2). Since no significant seasonal trend of $a_{CDOM}(350)$ appeared during this period, our results suggest that external influences such as Rhône River plume intrusion and mixing events control CDOM surface content and variability in Marseilles coastal area. At Arles station, Rhône River's $a_{CDOM}(350)$ annual mean ($2.42 \pm 1.05\,m^{-1}$) was likely higher than the marine one (Table 1). In the Rhône River plume, $a_{CDOM}(350)$ was 3–4 fold more important at 2 m compared at 5 m depth. Irradiation experiment on the Rhône River CDOM induced 30 and 60% losses of $a_{CDOM}(350)$ in T1 and T2 samples compared to T0 and dark control, respectively (Table 1).

In the Bay of Marseilles, the annual mean of $S_{CDOM}$ determined during this study was $0.019 \pm 0.003\,nm^{-1}$ at both depths which is consistent to that previously reported for October 1997 at the surface in vicinity of Rhône River mouth ($0.018 \pm 0.003\,nm^{-1}$) and for surface blue waters of the Gulf of Lions ($0.017 \pm 0.003\,nm^{-1}$) by Ferrari (2000). $S_{CDOM}$ extreme values (2 and 5 m) ranged from $0.014\,nm^{-1}$ on 25 November 2008 to $0.026\,nm^{-1}$ on 23 June 2008 (Table 1). Seasonal means of $S_{CDOM}$ were the lowest and comparable during fall and winter periods ($S_{CDOM}$ at 2 and 5 m $= 0.017 \pm 0.002\,nm^{-1}$) while during summer time $S_{CDOM}$ were significantly higher (U-Test, $p < 5\%$, $n = 3$–4) with seasonal mean value reaching $0.023 \pm 0.003\,nm^{-1}$ and $0.024 \pm 0.002\,nm^{-1}$ at 2 and 5 m depths, respectively. Spring means of $S_{CDOM}$ were in the middle of the range with $0.020 \pm 0.002\,nm^{-1}$ and $0.019 \pm 0.003\,nm^{-1}$ at 2 and 5 m depths, respectively.

The $S_{CDOM}$ annual mean of Rhône River samples (Arles Station) was lower ($0.017 \pm 0.001\,nm^{-1}$) than the marine one, whereas no apparent change in $S_{CDOM}$ value presented with a precision in the thousandth was observed after full sun exposure in T1 and T2 samples compared to T0 and dark control samples ($S_{CDOM} = 0.018\,nm^{-1}$, Table 1). However, it tended to increase during the irradiation experiment (from 0.0175 to $0.0180\,nm^{-1}$). In addition, this tendency was comforted by the slope ratio ($S_R$) values defined by Helms et al. (2008). $S_R$ consistently increased during irradiation in relation to the shifts in molecular weight. Indeed, between T0 (initial time) and T2 (final time), $S_R$ increased respectively from a terrestrial value (0.8) to a more typical coastal value ($1.36 \pm 0.05$). Interestingly, in the Rhône River plume $S_{CDOM}$ values at 2 m depth (0.017–$0.019\,nm^{-1}$) were strongly lower than at 5 m depth (0.021–$0.024\,nm^{-1}$) (Table 1).

The significant inverse relationship between salinity and $a_{CDOM}(350)$ for the shallowest depth studied (2 m) indicates a theoretical conservative behavior for surface CDOM absorbance (Fig. 3). The CDOM absorption mixing line established using all SOFCOM data at 2 m depth plus two data points acquired close to the Rhône Estuary in the Rhône River plume at 2 m depth in May 2008 has an intercept of $1.20 \pm 0.06\,m^{-1}$, which is in the range of that calculated for the Rhône River end member at Arles station ($2.42 \pm 1.05\,m^{-1}$) (Table 1). Moreover, when data from the Rhône River plume are excluded and all the SOFCOM data at both 2 and 5 m depths were used except the extreme values (23 September 2008 and 25 November 2008), another significant inverse relation was observed ($p < 1\%$, $n = 11$ at 2 m and $n = 12$ at 5 m), with $a_{CDOM}(350) = -0.032 \pm 0.007$ salinity $+1.33 \pm 0.25$, which is comparable to the previous calculation. However several data deviate significantly from the regression line. Points above the mixing line in Fig. 3 represent a net production of CDOM. The most important net production of CDOM was associated with low TOC concentration values (55–56 µMC) and with the lowest $S_{CDOM}$ ($0.014\,nm^{-1}$) values and occurred at both depths during a strong mixing event (25 November 2008). By contrast, the two points that fall far below the mixing line also present the highest salinities (38.4), high temperature (22 °C), high $S_{CDOM}$ values (0.021–$0.023\,nm^{-1}$), as well as moderately high surface irradiance [$E_s = 1.13\,\mu W\,cm^{-2}\,nm^{-1}$ for UVB (305 nm)] and were collected at the end of summer time (23 September 2008).

### 3.3 CDOM fluorescence

All the fluorescence peaks observed in this study in the Bay of Marseilles (SOFCOM Station) can be summarized from 3 samples showing contrasting hydrological conditions and collected on 23 June 2008 (Rhône plume intrusion), 23 September 2008 (photobleached water) and 25 November 2008 (well mixed water). On the other side, the fluorescence peaks determined from Rhône River samples (Arles Station) can be observed from the sample collected on 7 February 2009 and used for the irradiation experiment. EEMs for these samples are presented in Figs. 4 and 5 for SOFCOM and Arles samples respectively, while peaks intensities for all samples are reported in Table 2. During the fluorescence study period (i.e. June 2008–December 2008), in Marseilles' Bay, peak T (tryptophan-like, Ex/Em = 225/340 nm and 275/340 nm) was the major fluorescent peak present

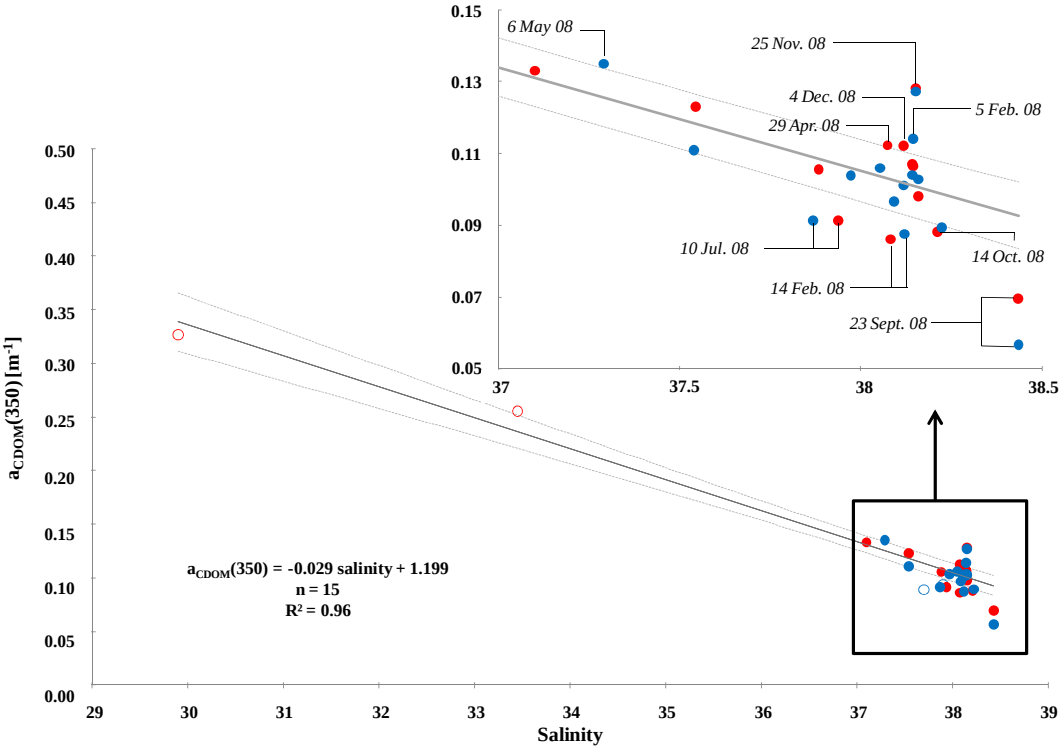


**Fig. 3.** Relationship between salinity and CDOM absorption at 350 nm (in $m^{-1}$) determined at SOFCOM station at 2 m (red circle, $n = 13$) and 5 m (blue circle, $n = 14$) depths. Data from Rhône Estuary stations collected in May 2008 during CHACCRA cruise at 2 m (red open circle, $n = 2$) and 5 m (blue open circle, $n = 2$) were also plotted. The mixing line (black line) with its confidence interval at 95% (dashed line) was established using all SOFCOM station data at 2 m depth ($n = 13$) plus Rhône Estuary stations (CHACCRA cruise data) at 2 m depth as well ($n = 2$).

($6.45 \pm 8.25$ QSU at 2 m depth and $1.94 \pm 0.93$ QSU at 5 m depth), followed by peak M (UVA marine humic-like, Ex/Em = 290–310/370–410 nm) with a mean value of $2.38 \pm 2.15$ QSU at 2 m depth and $1.74 \pm 1.65$ QSU at 5 m depth, and peak C (UVA humic-like Ex/Em = 320–360/420–460 nm) which was the least intense ($1.10 \pm 0.99$ QSU at 2 m depth and $0.93 \pm 0.95$ QSU at 5 m depth). Peak B (tyrosine-like, Ex/Em = 225/305 nm and 275/305 nm) was found only on 23 June 2008. The most striking feature about all EEMs is the lack of peak A (UVC humic-like, Ex/Em = 260/400–460 nm) for marine samples which was not the case for Rhône River samples. The Rhône River fluorescent CDOM had a strong terrestrial signature (humic-like components, peaks A and C). Indeed, the peak A was the major fluorescent peak with an annual mean value of $43.09 \pm 18.93$ QSU, followed by peaks C ($16.91 \pm 7.98$ QSU), and B ($7.96 \pm 0.82$ QSU). However this fluorescent terrestrial signature decreased strongly after irradiation exposure as suggest the irradiation experiment results (Fig. 5 and Table 2). Indeed at T1 and T2, the intensity of peaks A and C was divided by 3 and 4.5 respectively compared to the ones determined at T0 and dark control, while the intensity of peak B remained constant.

For Marseilles' Bay samples, maximum fluorescence intensities of peaks C, M and T (Table 2) at both depths occurred on 25 November 2008, during a strong mixing event enhanced by 12 consecutive days of Mistral wind and during a Rhône River plume extent event observed on 23 June 2008. For all other samples, all peak intensities were stable and low, especially in summer as observed on 10 July 2008 (despite the minor mixing event due to 3 consecutive days of Mistral wind) and 23 September 2008 (Table 2). The sample from 23 September 2008 showed a strong fluorescence signal in short Ex/Em wavelengths at both depths and possibly a slight signal of peak T as well (Fig. 4). This kind of signal at short wavelengths has been previously observed in strongly photobleached samples (P. Coble, unpublished data, 1998).

In contrast to the significant apparent relationship between surface $a_{CDOM}(350)$ and salinity, there was only a weak inverse relationship ($p < 5\%$, $n = 6$, $R^2 = 0.69$ and 0.67 for peaks C and M respectively, data not shown) between fluorescence of peaks C and M (Table 2) and salinity at 5 m depth when excluding the maximum values (25 November 2008). This result indicates that fluorescent CDOM character in the surface water is mainly driven by other processes than water mixing and thus highlights the dissimilar trends in CDOM absorption and fluorescence properties.

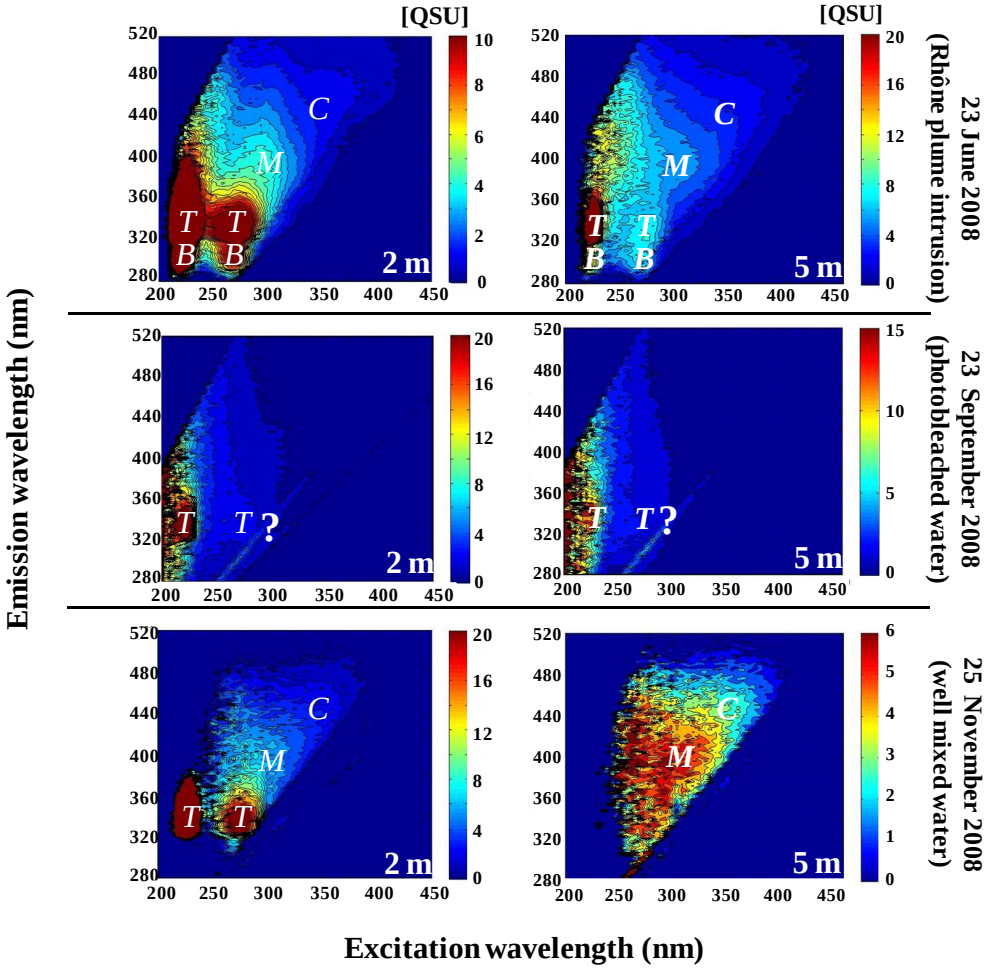


**Fig. 4.** 2-D EEM contour plots of CDOM (in QSU) collected in the Bay of Marseilles (SOFCOM station) at 2 (left panels) and 5 m depths (right panels) on 23 June (upper panels), 23 September (middle panels) and 25 November 2008 (bottom panels). These spectra illustrated fluorescent peaks positions observed during this study. Corresponding peaks fluorescence intensities are reported on Table 2. On middle panels, question marks indicate a possible slight signature of the peak T.

HIX and BIX values determined for marine (SOFCOM) and freshwater (Arles) samples are presented on Table 3. During the study period, for SOFCOM samples at both depths, HIX values were low and variable with $0.84 \pm 0.38$ and $0.90 \pm 0.35$ at 2 m and 5 m depths, respectively, while BIX values were high and stable: $1.10 \pm 0.17$ and $1.09 \pm 0.05$, respectively. These results suggest a predominantly autochthonous origin of DOM in surface marine waters. BIX maximum values were observed at 2 m depth on 23 June 2008 and 25 November 2008 while the lowest one was observed on 7 July 2008 at 2 m depth. This date corresponded also at the maximum values observed at both depths for HIX. At Arles station, Rhône River CDOM likely contains compounds of higher molecular weight compared to marine CDOM. Indeed, high HIX values ($4.85 \pm 1.55$) and low BIX values ($0.74 \pm 0.05$) suggest a predominantly allochthonous origin of DOM. The high variability of HIX (CV = 32%), which is the ratio of $H/L$, for these freshwater samples came from the variability concerning the presence of complex high molecular weight components (i.e., $H$, CV = 41%), while low molecular weight components part remained more steady (i.e., $L$, CV = 13%). The Rhône River irradiation experiment shows a strong decrease in HIX at T1 and T2 triggered by $H$ value decreased ($H = 1433$, 1326, $810 \pm 44$ and $426 \pm 15$ QSU at T0, Dark control, T1 and T2, respectively) while corresponding BIX remained constant (Table 3), due to an alteration in similar proportion of humic-like components, compared to T0 and dark control. Such results, strong decrease of HIX (∼50%) coupled to a constant BIX between T0 (initial time) and T2 (final time) underline the higher photosensitivity feature of high molecular weight DOM (i.e. humic-like components) compared to low molecular weight DOM (i.e. protein-like components) (Table 2).

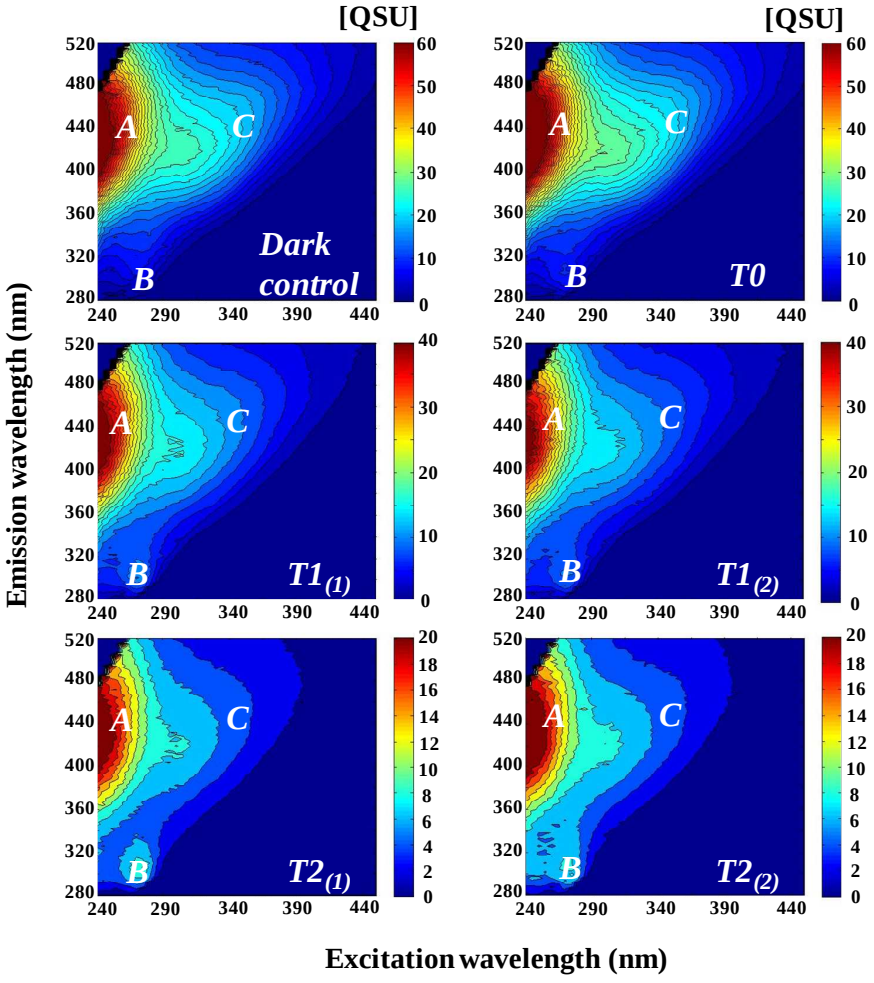


**Fig. 5.** 2-D EEM contour plots of CDOM (in QSU) collected from Rhône River sample, before (T0: upper panel right), and after a full sun exposure of 8 (T1: middle panels) and 20 h (T2: bottom panels) using solar simulator. Color-bars' scales are different. Dark control is indicated in upper panel (left). Corresponding peaks fluorescence intensities are reported on Table 2.

Shape of normalized emission spectra to the corresponding maximum emission intensity can provide information on the nature as well as on biogeochemical processes affecting DOM. Normalized emission spectra of peaks C and M were both determined (Fig. 6) for the 3 marine samples influenced by contrasted hydrological conditions (23 June 2008, 23 September 2008 and 25 November 2008) (Fig. 6). Additional normalized emission spectra of the peak C corresponding to T0 (initial time), dark control and T2 (final time) of the Rhône River sample irradiation experiment were also plotted on Fig. 6. At SOFCOM station, both humic-like peaks (C and M) presented the same pattern at both depths, with the broadest emission spectra observed on photobleached water samples (23 September 2008) followed by the Rhône River intrusion one (23 June 2008) while the narrowest spectra were determined during the mixing event (25 November 2008). For the Rhône River, emission spectra of peak C were likely broader than the SOFCOM ones. Interestingly, after irradiation (i.e. T2 sample) corresponding emission spectra were widening towards the longer Em wavelengths compared to T0 and Dark control.

## 4 Discussion

### 4.1 Evidence for a biological origin of CDOM at SOFCOM station

Despite the low and quite stable values of $a_{CDOM}(350)$ determined in surface waters of the Bay of Marseilles, the significant inverse linear relationship observed at both depths between $a_{CDOM}(350)$ and salinity illustrated a theoretical conservative behavior of surface CDOM in this area. This represents the first report of the potential biogeochemical influence of the Rhône River plume in this oligotrophic coastal area. Such a strong significant inverse relationship between salinity and fluorescent/absorbant CDOM is

**Table 2.** Fluorescence intensity (in QSU) and peak positions of tyrosine-like (B), tryptophan-like (T), UVA humic-like (C), marine humic-like (M) and UVC humic-like (A) determined at SOFCOM (2 and 5 m depths) and Arles station (Rhône and Rhône irradiation experiment: Rhône Irrad. Exp.) at 2 m depth. Emission ranges represent the band from which a mean of fluorescence intensity was calculated. (nd = not determined).

| | Peak fluorescence intensity (QSU) | | | | | | | | | |
|---|---|---|---|---|---|---|---|---|---|---|
| | B | | C | | M | | T | | A | |
| | Ex/Em (nm) = 275/300–310 | | Ex/Em (nm) = 350/430–450 | | Ex/Em (nm) = 300/380–400 | | Ex/Em (nm) = 275/330–350 | | Ex/Em (nm) = 260/430–440 | |
| End-member | 2 m | 5 m | 2 m | 5 m | 2 m | 5 m | 2 m | 5 m | 2 m | 5 m |
| SOFCOM 9 Jun 2008 | nd | nd | 0.56 ± 0.04 | 0.57 ± 0.04 | 1.02 ± 0.06 | 1.24 ± 0.08 | 1.70 ± 0.18 | 1.74 ± 0.13 | nd | nd |
| SOFCOM 23 Jun 2008 | 11.06 ± 0.81 | 3.51 ± 0.67 | 1.40 ± 0.06 | 1.54 ± 0.08 | 4.34 ± 0.13 | 2.73 ± 0.12 | 14.13 ± 1.57 | 3.78 ± 0.20 | nd | nd |
| SOFCOM 10 Jul 2008 | nd | nd | 0.49 ± 0.03 | 0.51 ± 0.04 | 0.85 ± 0.06 | 0.96 ± 0.06 | 1.25 ± 0.13 | 1.46 ± 0.09 | nd | nd |
| SOFCOM 23 Sep 2008 | nd | nd | 0.57 ± 0.04 | 0.42 ± 0.03 | 1.26 ± 0.07 | 0.90 ± 0.09 | 2.77 ± 0.20 | 1.87 ± 0.09 | nd | nd |
| SOFCOM 14 Oct 2008 | nd | nd | nd | 0.27 ± 0.03 | nd | 0.55 ± 0.08 | 1.30 ± 0.18 | 1.58 ± 0.17 | nd | nd |
| SOFCOM 25 Nov 2008 | nd | nd | 2.99 ± 0.18 | 2.85 ± 0.22 | 5.82 ± 0.49 | 5.11 ± 0.52 | 21.94 ± 2.66 | nd | nd | nd |
| SOFCOM 4 Dec 2008 | nd | nd | 0.59 ± 0.04 | 0.34 ± 0.03 | 0.98 ± 0.05 | 0.71 ± 0.07 | 2.08 ± 0.18 | nd | nd | nd |
| Mean | – | – | 1.10 | 0.93 | 2.38 | 1.74 | 6.45 | 1.94 | – | – |
| SD | – | – | 0.99 | 0.95 | 2.15 | 1.65 | 8.25 | 0.93 | – | – |
| Rhône (Arles) (Jun–Dec 2008, $n = 6$) | 7.96 ± 0.82 | – | 16.91 ± 7.98 | – | nd | – | nd | – | 43.09 ± 18.93 | – |
| Rhône Irrad. Exp. T0 | 8.99 ± 0.76 | – | 21.35 ± 0.33 | – | nd | – | nd | – | 56.30 ± 0.72 | – |
| Rhône Irrad. Exp. Dark control | 7.12 ± 0.50 | – | 19.71 ± 0.21 | – | nd | – | nd | – | 53.60 ± 1.56 | – |
| Rhône Irrad. Exp. T1 duplicate | 10.24 ± 0.65 | – | 9.67 ± 0.52 | – | nd | – | nd | – | 31.36 ± 1.59 | – |
| Rhône Irrad. Exp. T2 duplicate | 8.34 ± 0.58 | – | 4.57 ± 0.21 | – | nd | – | nd | – | 16.77 ± 0.22 | – |

**Table 3.** Values of Humification (HIX; Zsolnay et al., 1999), Biological (BIX; Huguet et al., 2009) indices and the ratio of marine humic-like (Ex/Em = 300/380–400 nm) to humic like (Ex/Em = 350/430–450 nm) (M/C) fluorescence determined at SOFCOM (2 and 5 m depths) and Arles station (Rhône and Rhône irradiation experiment: Rhône Irrad. Exp.) at 2 m depth. (nd = not determined).

| | HIX | | BIX | | M/C | |
|---|---|---|---|---|---|---|
| End-member | 2 m | 5 m | 2 m | 5 m | 2 m | 5 m |
| SOFCOM 9 June 2008 | 0.93 | 0.96 | 1.04 | 1.00 | 1.81 | 2.17 |
| SOFCOM 23 June 2008 | 0.42 | 1.22 | 1.34 | 1.10 | 3.11 | 1.77 |
| SOFCOM 10 July 2008 | 1.32 | 1.35 | 0.86 | 1.09 | 1.74 | 1.89 |
| SOFCOM 23 September 2008 | 1.04 | 0.96 | 1.02 | 1.06 | 2.22 | 2.12 |
| SOFCOM 14 October 2008 | nd | 0.27 | nd | 1.12 | nd | 2.08 |
| SOFCOM 25 November 2008 | 1.01 | 0.77 | 1.26 | 1.15 | 1.95 | 1.79 |
| SOFCOM 4 December 2008 | 0.35 | 0.76 | 1.05 | 1.11 | 1.68 | 2.08 |
| Mean | 0.84 | 0.90 | 1.10 | 1.09 | 2.09 | 1.99 |
| SD | 0.38 | 0.35 | 0.17 | 0.05 | 0.54 | 0.17 |
| Rhône (Arles) (June–December 2008, $n = 6$) | $4.85 \pm 1.55$ | – | $0.74 \pm 0.05$ | – | nd | – |
| Rhône Irrad. Exp. T0 | 6.19 | – | 0.66 | – | nd | – |
| Rhône Irrad. Exp. Dark control | 6.41 | – | 0.69 | – | nd | – |
| Rhône Irrad. Exp. T1 duplicate | $4.10 \pm 0.15$ | – | $0.67 \pm 0.01$ | – | nd | – |
| Rhône Irrad. Exp. T2 duplicate | $3.21 \pm 0.10$ | – | $0.67 \pm 0.02$ | – | nd | – |

typically observed in coastal areas subjected to high river inputs (Blough et al., 1993; Green and Blough, 1994; Nelson and Guarda, 1995; Højerslev et al., 1996; Nieke et al., 1997; Vodacek et al., 1997; Seritti et al., 1998; Del Castillo et al., 2000; Ferrari, 2000; Stedmon et al., 2000).

By contrast, the lack of correlation between salinity and fluorescence intensities of peaks C and M at 2 m depth (excluding the maximum values, 25 November 2008) and the only weakly significant correlation observed for 5 m depth samples suggest that the Rhône River plume is not a dominant source of fluorescent CDOM in the Bay of Marseilles. Fluorescent CDOM content in surface waters is likely driven by others processes such as in situ production or photooxidation rather than water mixing as already hypothesized by Vignudelli et al. (2004) for coastal waters of the northern Tyrrhenian Sea (Italy). The first of these processes is photobleaching, which has more impact on fluorescence than on absorbance properties (Moran et al., 2000; Nieto-Cid et al., 2006). This phenomenon is likely observed during water stratification, especially during spring and summer periods when UV irradiance is high (Table 1). Therefore, it is very likely that samples collected at the end of summer period (23 September 2008), were strongly photobleached explaining the lack (loss) of peaks M and C (Fig. 4). This assumption would be consistent with high $S_{\mathrm{CDOM}}$ coupled to low $a_{\mathrm{CDOM}}(350)$ values (Table 1) that fell beneath the mixing line in Fig. 3, and suggest a net loss of CDOM at this time (i.e. on 10 July 2008 and 23 September 2008). In addition, the lowest specific absorption coefficient ($a_{\mathrm{CDOM}}(350)/\mathrm{TOC} = 0.0010$ and 0.0009 at 2 and 5 m depths respectively) was determined at this date too. In situ production is another process that may modify CDOM fluorescence character. Indeed, phytoplankton production (Romera-Castillo et al., 2010), zooplankton grazing (Coble et al., 1998) and bacterial activity (Stedmon and Markager, 2005) may induce production of fluorescent CDOM through by-products, especially peaks B, T, and M. Primary production and bacterial activity promoted by the Rhône River plume intrusion event rich in nutrients (Chl-*a* concentration $>1\,\mu\mathrm{g\,l^{-1}}$; on 6 May 2008 and 23 June 2008) may have produced fluorescent CDOM. Finally, the strong mixing observed on 25 November 2008 sample could have injected relatively aged CDOM from the bottom to the surface as well as nutrients and thus explain an increase of surface CDOM concentrations (Coble et al., 1998; Nelson et al., 2004, Nieto-Cid et al., 2006). Moreover, this humic CDOM showed the highest specific absorption coefficient ($a_{\mathrm{CDOM}}(350)/\mathrm{TOC} = 0.0024$ and 0.0023 at 2 and 5 m depths, respectively) at both depths and that could explain the highest $a_{\mathrm{CDOM}}(350)$ determined at this date.

Surface CDOM content in the Bay of Marseilles results, therefore, from the combination of several processes which differentially affect its fluorescence and absorbance properties. In any case, our results put forward that CDOM properties in this area is much more affected by autochthonous production induced by the Rhône River plume intrusion than by the original Rhône River DOM (i.e. system truly non-conservative).

In Marseilles Bay, during the one year survey, surface CDOM exhibited very low and stable $a_{\mathrm{CDOM}}(\lambda)$ and high variability of $S_{\mathrm{CDOM}}$, highest values being observed during summer time. Generally such signals as well as low surface TOC concentration and Chl-*a* concentration are

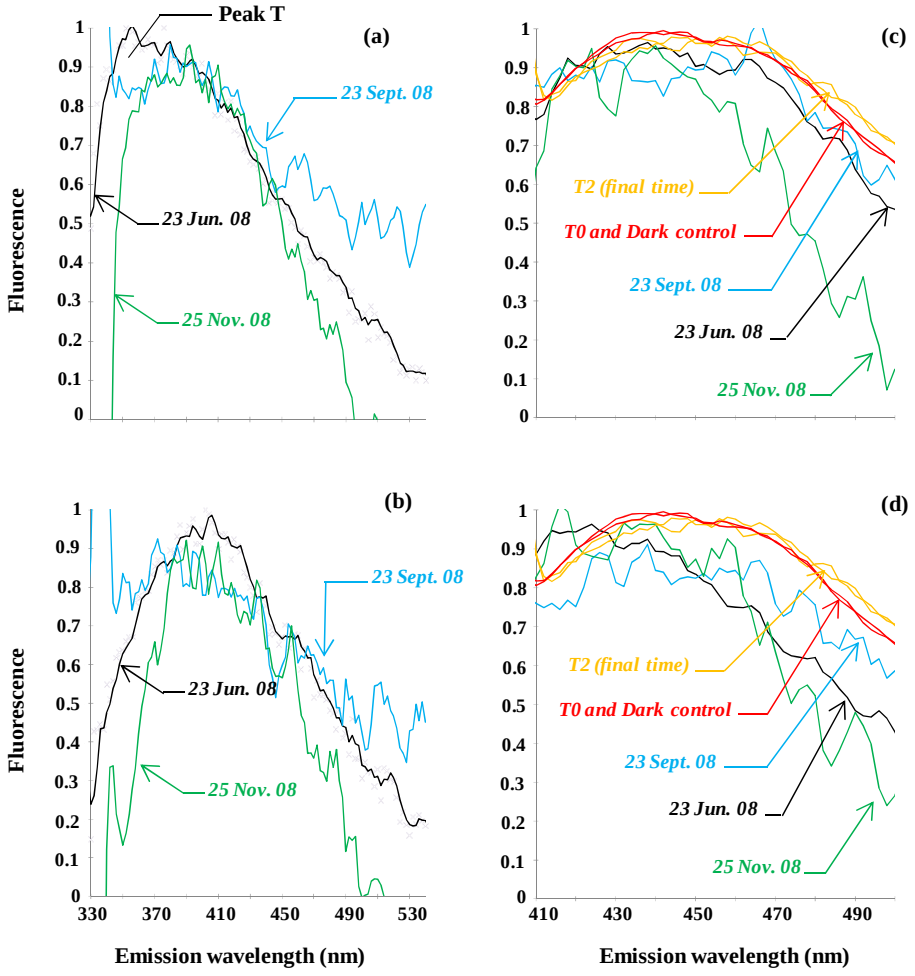


**Fig. 6.** Normalized emission spectra of peak M at Ex = 300 nm (**a** and **b**) and peak C at Ex = 350 nm (**c** and **d**) acquired at SOFCOM station on 23 June (Rhône plume intrusion sample, black solid line), 23 September (photobleached sample, blue solid line) and 25 November 2008 (well mixed sample, green solid line) at 2 (upper panel) and 5 m (bottom panel) depths. Normalized emission spectra of peak C determined at T0, dark control (red solid line) and T2 (duplicate, orange solid line) of the irradiation experiment performed on Rhône River sample collected on 7 February 2009 at 2 m depth were also plotted on both panels **(c)** and **(d)**. These emission spectra were normalized to the maximum emission intensity in the range 380–400 nm for the peak M and 430–450 nm for the peak C. These spectra were smoothed by a moving average order 3 which imposes a red shifted of 5 nm.

observed offshore (Blough and Del Vecchio, 2002) or in an oligotrophic coastal area not influenced by river inputs. High $S_{CDOM}$ could reflect either CDOM photobleaching if $a_{CDOM}(\lambda)$ is low as observed during summer (10 July 2008 and 23 September 2008) or fresh biological CDOM production in surface waters if $a_{CDOM}(\lambda)$ is high as observed on 23 June 2008. By contrast, low $S_{CDOM}$ with high $a_{CDOM}(\lambda)$ as observed on 25 November 2008 suggest the presence of aged CDOM in surface that could be the consequence of the strong mixing of deep water that was reported at this period.

Concerning CDOM fluorescence properties, our study showed the dominance of recent autochthonous compounds (peak T, BIX >1) and extremely low values of humic substances (peaks C and M, HIX≈1) within marine surface CDOM pool. Fluorescence intensity of peak T observed on all dates (except on 23 June 2008 and 25 November 2008) at 2 and 5 m depths (Table 2) was in accordance to that reported in surface Ise Bay in the Pacific coastal area (Yamashita and Tanoue, 2003). Interestingly, during Rhône River plume intrusion and mixing events in Marseilles Bay, fluorescence intensity of peak T was one order of magnitude higher at 2 m depth (Table 2). The origins of peaks T and M have been attributed to planktonic activity (Determann et al., 1998; Myklestad, 2000; Nieto-Cid et al., 2006; Romera-Castillo et al., 2010) while the origin of peak C is known to be terrestrial and thus coming from freshwater inputs (Sierra et al., 1997, 2005; Komada et al., 2002). However, peak C which is relatively abundant in deep waters could also originate from the humification of marine DOM and thus may reach surface waters during upward mixing events (Coble et al., 1998; Parlanti

et al., 2000). Mayer et al. (1999) in two Maine estuaries (Atlantic Ocean) observed that seawater samples tended to show higher tyrosine (peak B) while upstream samples were richer in tryptophan (peak T). These observations are in accordance with our results: presence of peak T and absence of peak B in coastal waters (except on 23 June 2008). According to Lakowicz (2006) and Mayer et al. (1999) tyrosine fluorescence is quenched by tryptophan in folded proteins. This implies that the tryptophan observed at SOFCOM station is probably bounded in proteins rather than in free dissolved form.

To reinforce the hypothesis of the biological source of surface fluorescent CDOM in the Bay of Marseilles, 3 fluorescence indices were also calculated including HIX, BIX and M/C peaks ratio (Table 3). Our results showed low and variable values of HIX and high constant values of BIX, suggesting a predominantly autochthonous origin of DOM and the presence of organic matter freshly released in marine surface waters. The lack of terrestrial signature of CDOM is surprising particularly during Rhône River plume intrusion, easily detected on 23 June 2008 from remote sensing observations. At this date, the lowest HIX value was observed at 2 m depth (0.42) while it was around 3 fold more important at 5 m depth (1.22). The efficiency of photo-oxidation process in surface layer could explain such different HIX values between 2 and 5 m depths. Indeed, a significant proportion, as high as 96%, of CDOM from freshwater (i.e. humic material) might be destroyed during long term exposure to solar radiation (Vähätalo and Wetzel, 2004). Grzybowski (2000) estimated riverine CDOM to be 10 fold more sensitive than coastal CDOM to photobleaching, with the effects of this process being detectable after only 6 h of exposure under natural sunlight. During the eastward spreading of the buoyant Rhône River plume on surface marine waters, an important part of the terrestrial CDOM pool could be removed, as well as a part of the autochthonous CDOM freshly produced, if any, due to photobleaching (Fig. 5) (Vodacek et al., 1997; Del Castillo et al., 1999). Thus, photobleaching could explain the lack of terrestrial fluorescence signature in this coastal area during Rhône River plume intrusion.

High and constant BIX values at both depths illustrated the omnipresence of the peak M, characterizing an autochthonous biological activity which was slightly more important at 2 m than 5 m depth (except on 10 July 2008 during a mixing event), particularly under Rhône River plume influence (23 June 2008) (Table 3). The competing process of photobleaching probably hid a part of this biological activity especially in the surface waters. The highest BIX values at 2 m depth determined on 23 June 2008 and 25 November 2008 corresponded respectively to an important Rhône River plume intrusion containing freshly produced CDOM and to a strong water column mixing that may injected humic CDOM in surface waters. The M/C ratio reflects the relative amount of new (marine) to old (terrestrial) CDOM. On 23 June 2008, higher values found at 2 m relative to 5 m depth (Table 3) reinforces the hypothesis that biological activity and/or photobleaching are more important in the surface layer.

The discrimination between marine phytoplankton and bacteria as the predominant biological source of peak T can be assessed through spectral analyses of this peak according to the criteria of Determann et al. (1998). Normalized emission spectra at Ex = 230 nm at both depths (Fig. 7b and d) exhibited peaks position in the 325–345 nm range while the one of free dissolved L-tryptophan used as standard was around 360 nm, in agreement with the findings of Determann et al. (1998). A weak second band at 300 nm, specific to phytoplankton species, was only observed for samples from 23 June 2008 (black solid line) and 23 September 2008 (blue solid line) and was more pronounced at 5 m than at 2 m. In normalized excitation spectra at Em = 340 nm (Fig. 7a and c), the main absorption band in the 220–230 nm range was clearly red shifted around the range 230–235 nm on 9 June 2008 (orange solid line) at both depths and on 10 July 2008 (red solid line) at 5 m depth, as observed by Determann et al. (1998) with bacteria cultures. Moreover, at these dates and depths another absorption band (specific to bacteria) in the range 275–280 nm was observed while at the other dates a signal more or less constant was observed. Therefore, such results perhaps illustrated a dominant phytoplankton origin for tryptophan at both depths on 23 June 2008 and 23 September 2008 while tryptophan had a dominant bacterial origin on 9 June 2008 at both depths and on 10 July 2008 at 5 m depth.

Assessing the predominant biological origin for the other dates studied regarding emission and excitation spectra of tryptophan results is not straightforward, possibly due to an equal contribution of phytoplankton and bacteria origin to the tryptophan content. It is important to note that these results obtained on spectral analyses of peak T are extrapolated from those obtained from in vitro experiments (Determann et al., 1998) and thus should be taken to some extent with caution. Interestingly the results of this discrimination were logical regarding the hydrological context. Indeed, dominant phytoplankton origin of tryptophan took place during bloom periods enhanced by nutrients inputs through an intrusion of the Rhône River plume (23 June 2008) and or through a mixing (23 September 2008), whereas dominant bacteria origin of tryptophan took place (9 June 2008 and 10 July 2008) after or during bloom events. This ecological succession (phytoplankton/bacteria) was in a good agreement with the work of Lemée et al. (2002), which highlights the net heterotrophic character of bacteria in the upper layer of the northwestern Mediterranean Sea.

### 4.2 Seasonal evolution of surface CDOM at SOFCOM station

The results taken as a whole allow seasonal features of the surface CDOM content to be established for the Bay of Marseilles. In spring and summer time, when the water column

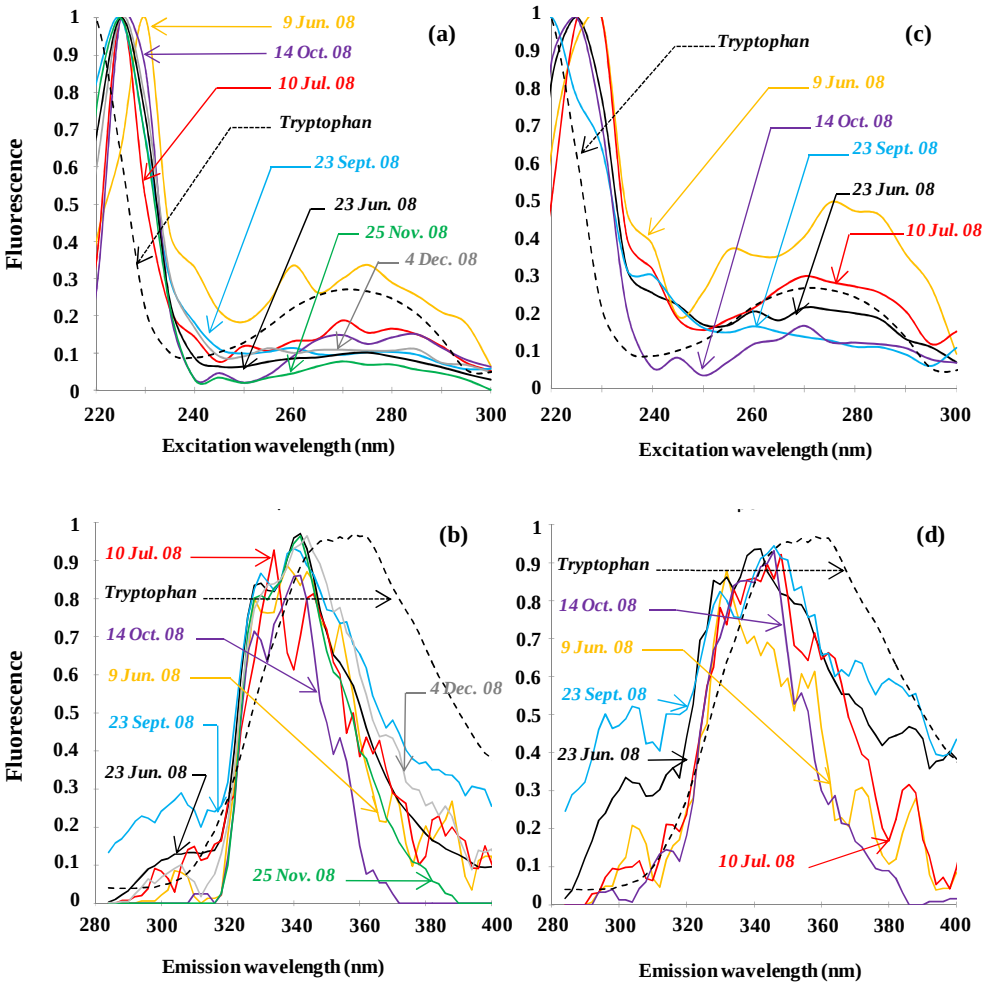


**Fig. 7.** Normalized excitation and emission spectra of peak T collected on 9 June (orange solid line), 23 June (black solid line), 10 July (red solid line), 23 September (blue solid line), 14 October (purple solid line), 25 November (green solid line) and 4 December 2008 (grey solid line). All these spectra are compared to a standard solution (75 µg $l^{-1}$ of free dissolved L-tryptophan, >98%, Sigma-Aldrich, black dashed line). **(a)** and **(c)** excitation spectra with Em = 340 nm at 2 and 5 m depth respectively, normalized to the maximum value intensity in the 220–240 nm range. **(b)** and **(d)** emission spectra with Ex = 230 nm at 2 and 5 m depth respectively, normalized to the maximum value intensity in the 320-360 nm range. In order to reduce the noise, all these emission-excitation spectra were smoothed by a moving average order 3 which imposes a red shifted of 5 nm.

becomes stratified, freshwater intrusions of the Rhône River plume were easily identifiable by lowered salinities (Fig. 2). The high nutrient content of this buoyant plume enhanced marine primary production in surroundings surface marine waters (Cruzado and Velasquez, 1990; Pujo-Pay et al., 2006; Joux et al., 2009) (Fig. 8). This would be consistent with our observations on 6 May 2008 and 23 June 2008. The time scale of its transport to the Bay of Marseilles under solar radiation certainly play a major role in the state of development of primary production associated with bacteria communities and also in the terrestrial CDOM content and properties (Fig. 8). At the end of spring, on 9 June 2008 (post blooms period), the biological origin of the major fluorescent peak released (peak T, tryptophan-like) was logically dominated by bacteria at 2 and 5 m depths.

At the beginning of summer (23 June 2008) during an important surface extent of the Rhône River plume in the Bay of Marseilles, CDOM content showed a high absorption coefficient along with the highest spectral slope (Table 1) underlining the biological origin of CDOM. In addition, high fluorescence intensities for all peaks (T, M, C, and B) (Table 2), as well as fluorescence indices values (HIX, BIX and M/C) (Table 3) indicated a well developed surface biological activity producing fresh fluorescent CDOM. Moreover, at this period, tryptophan-like material originated from phytoplankton at both depths.

Two weeks after this important bloom, on 10 July 2008, bacteria dominated the biological input of tryptophan at 5 m depth. On this date, the autochthonous production of CDOM was weak while $S_{CDOM}$ was high despite a minor mixing

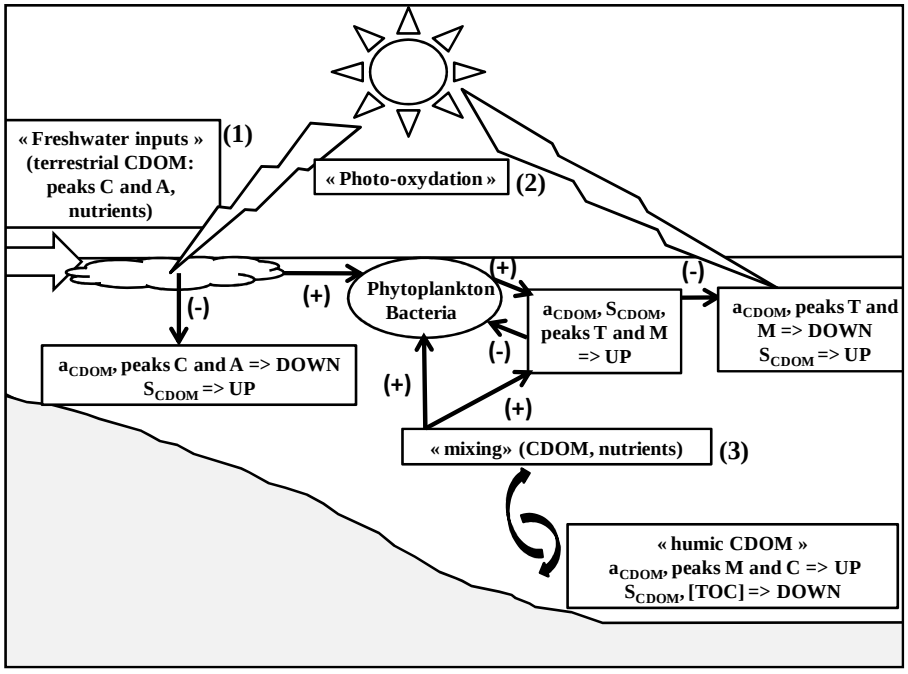


**Fig. 8.** Synthesis of processes (Rhône River plume intrusion (1), photo-oxydation of CDOM (2) and water mixing (3)) driving surface CDOM dynamic and content in the Bay of Marseilles and their direct and indirect effects (positive or negative) on CDOM optical properties.

event that probably injected nutrients and humic CDOM into surface waters (Fig. 8). This could explain the significant values of HIX and BIX. Nevertheless, low $a_{CDOM}(350)$ coupled to a high $S_{CDOM}$ also point out the efficiency of photobleaching effect of CDOM and could explain its net loss observed on 10 July 2008 at both depths.

During the summer time, under any influence of Rhône River plume, photobleaching appeared as a significant sink for CDOM (Fig. 8). This process was most clearly illustrated at the end of summer time, on 23 September 2008, with respect to the quality and quantity of CDOM content. Indeed, on 23 September 2008 the warm and salty water mass present had persisted at the surface since late July (Fig. 2) and had thus spent 6–8 weeks exposed to high UV radiation. Values of $a_{CDOM}(350)$ exhibited minima at both depths and spectral slopes were high especially at 5 m depth where the water was saltiest (Table 1). Moreover, EEMs illustrated a strong signal of fluorescence in short Ex/Em wavelengths (Fig. 4), which was attributed to photobleaching. Thus, it was logical that the most important net loss of CDOM due to photobleaching appeared at the end of summer time just before fall mixing.

Finally, during fall, on 25 November 2008, 12 consecutive days of Mistral wind enhanced strong deep mixing that put nutrients back in the surface waters as well humic CDOM, from bottom water (Coble, 1998; Sierra et al., 1997, 2005; Komada et al., 2002) (Fig. 8). The maximum of value for peak C was observed on this date (Table 2). Maximum values for autochthonous humic CDOM (peak M) were also observed at this time, probably of bacterial origin (Nieto-Cid et al., 2006). Therefore, the inputs of humic CDOM (peaks C and M) explain the highest $a_{CDOM}(350)$ and the lowest spectral slope of CDOM observed at both depths during this period.

## 5 Conclusions and perspectives

This study highlights the low surface CDOM content in the Bay of Marseilles through $a_{CDOM}(350)$ and TOC concentration values. Stable and very low annual mean value of $a_{CDOM}(350)$ prevents the establishment of a seasonal trend, while $S_{CDOM}$ values were significantly higher during the summer time period and thus could reflect either photobleaching or biological production of CDOM in the surface waters. Values of $a_{CDOM}(350)$ in this well-urbanized coastal area were comparable to those usually found in the open ocean. The different fluorescent peaks identified in this study show the predominance of protein-like component, peak T, and marine humic-like component, peak M. The omnipresence of these fluorescent peaks is related to the biological activity occurring mainly in the surface waters of the Bay of Marseilles. The very low content in UVA humic-like peak C demonstrates the quasi absence of terrestrial or aged material within surface fluorescent CDOM composition. Our observations show that the optical properties of water in the Bay of Marseilles are governed mostly by phytoplankton with their accompanying by-products whereas the sporadic terrigeneous influence is negligible. Therefore, this coastal

system may be considered as truly non-conservative. In such oligotrophic environment, it appears that fluorescence analyses gather more pertinent information on CDOM composition and dynamics than absorbance analyses.

This study points out for the first time that the surface waters of the Bay of Marseilles are influenced by episodic events of the eastward extent of the Rhône plume. In this coastal oligotrophic area, these events enhance surface primary production and bacterial activity in surroundings waters which in turn increase the surface CDOM production. This source of CDOM appears more efficient at 2 m and during water stratification. On the other side, photobleaching acts as a significant sink of CDOM in summer, whereas the mixing of bottom waters containing humic CDOM may enrich the surface waters.

From the results presented in this work, it appears clearly that the Rhône River plume intrusions as well as mixing of the water column have a significant impact on the biogeochemical cycles in the Bay of Marseilles. Determining photobleaching rates of surface CDOM appears also as an important issue. A higher temporal determination of these processes in this coastal area will enable a better understanding of the biogeochemical/physical processes driving the CDOM distribution, dynamics and fate in the Marseilles Bay and will shed light on some features, not observed in this study, such as interseasonal trend of CDOM, and relationships between fluorescence, absorbance and DOC concentration, commonly observed in coastal area.

*Acknowledgements.* This work was supported by the French CHACCRA program (ANR-06-VULN-001 PI: C. Rabouille), INSU/CNRS as well as Conseil Général des Bouches du Rhône (CG13) and Pôle Mer PACA funding UVPACA project (PI: B. Charrière). This study partly contributes to "Sea Explorer" project supported by the French "Fond de Compétitivité des Entreprises" and Pôle Mer PACA. We are very grateful to the crews of the R/V *Antedon II* and *Tethys II* for their excellent service at sea and the SO-COM staff for providing CTD data from SOFCOM station and for collecting Rhône River samples at Arles station. We thank IFREMER for providing ocean color data through the website http://www.ifremer.fr/nausicaa/medit/index.htm. We are grateful to M. Goutx for the use of the Hitachi spectrofluorometer. Ph.D. scholarship to J. Para was provided by PACA region, whereas visiting professor fellowship to P. Coble was provided by Université de la Méditerranée. We thank the anonymous reviewers for advices that greatly improved the quality of this manuscript.

Edited by: K. Suzuki


The publication of this article is financed by CNRS-INSU.

## References

Amiotte-Suchet, P., Probst, J. L., and Ludwig, W.: Worldwide distribution of continental rock lithology: implications for the atmospheric/soil $CO_2$ uptake by continental weathering and alkalinity river transport to the ocean, Global Biogeochem. Cy., 17, 1038, doi:10.1029/2002GB001891, 2003.

Arnoux-Chiavassa, S., Rey, V., and Fraunié, P.: Modeling 3D Rhône river plume using a higher order advection scheme, Oceanol. Acta, 26, 299–309, 2003.

Azam, F., Fenchel, T., Field, J. G., Gray, J. S., Meyer-Reil, L. A., and Thingstad, F.: The ecological role of water-column microbes in the sea, Mar. Ecol-Prog. Ser., 10, 257–263, 1983.

Babin, M., Stramski, D., Ferrari, G. M., Claustre, H., Bricaud, A., Obolensky, G., and Hoepffner, N.: Variations in the light absorption coefficients of phytoplankton, non-algal particles, and dissolved organic matter in coastal waters around Europe, J. Geophys. Res., 108(C7), 1–20, 2003.

Belzile, C., Roesler, C. S., Christensen, J. P., Shakhova, N., and Semiletov, I.: Fluorescence measured using the WETStar DOM fluorometer as a proxy for dissolved matter absorption, Estuar. Coast. Shelf S., 67, 441–449, 2006.

Blough, N. V. and Del Vecchio, R.: Chromophoric DOM in the Coastal Environment, in: Biogeochemistry of Marine Dissolved Organic Matter, edited by: Hansell, D. A. and Carlson, C. A., Academic Press, San Diego, 509–540, 2002.

Blough, N. V., Zafiriou, O. C., and Bonilla, J.: Optical absorption spectra of water from the Orinoco River outflow: Terrestrial input of colored organic matter to the Caribbean, J. Geophys. Res., 98(C2), 2271–2278, 1993.

Brasseur, P., Beckers, J. M., Brankart, J. M., and Schoenauen, R.: Seasonal temperature and salinity fields in the Mediterranean Sea: climatological analyses of a historical data set, Deep-Sea Res. Pt. I, 43, 159–192, 1996.

Bricaud, A., Morel, A., and Prieur, L.: Absorption by dissolved organic matter of the sea (yellow substance) in the UV and visible domains, Limnol. Oceanogr., 26, 43–53, 1981.

Broche, P., Devenon, J. L., Forget, P., De Maistre, J. C., Naudin, J. J., and Cauwet, G.: Experimental study of the Rhone plume. Part I: physics and dynamics, Oceanol. Acta, 21, 725–738, 1998.

Coble, P. G.: Characterization of marine and terrestrial DOM in seawater using excitation emission matrix spectroscopy, Mar. Chem., 51, 325–346, 1996.

Coble, P. G.: Marine optical biogeochemistry: the chemistry of ocean color, Chem. Rev., 107, 402–418, 2007.

Coble, P. G., Green, S. A., Blough, N. V., and Gagosian, R. B.: Characterisation of dissolved organic matter in the Black Sea by fluorescence spectroscopy, Nature, 348, 432–435, 1990.

Coble, P. G., Schultz, C. A., and Mopper, K.: Fluorescence contouring analysis of DOC intercalibration experiments samples: a comparison of techniques, Mar. Chem., 41, 173–178, 1993.

Coble, P. G., Del Castillo, C. E., and Avril, B.: Distribution and optical properties of CDOM in the Arabian Sea during the 1995 southwest monsoon, Deep-Sea Res. Pt. II, 45, 2195–2223, 1998.

Cristofanelli, P. and Bonasoni, P.: Background ozone in the southern Europe and Mediterranean area: influence of the transport processes, Environ. Pollut., 157, 1399–1406, 2009.

Cruzado, A. and Velasquez, Z. R.: Nutrients and phytoplankton in the Gulf of Lions, Cont. Shelf. Res., 10, 931–942, 1990.

D'Sa, E. J., Steward, R. G., Vodacek, A., Blough, N. V., and

Phinney, D.: Determining optical absorption of colored dissolved organic matter in seawater with a liquid capillary waveguide, Limnol. Oceanogr., 44(4), 1142–1148, 1999.

Dafner, E. V., Sempéré, R., and Bryden, H. L.: Total organic carbon distribution and budget through the Strait of Gibraltar in April 1998, Mar. Chem., 73, 233–252, 2001.

De Souza-Sierra, M. M., Donard, O. F. X., Lamotte, M., Belin, C., and Ewald, M.: Fluorescence spectroscopy of coastal and marine waters, Mar. Chem., 47, 127–144, 1994.

Del Castillo, C. E., Coble, P. G., Morell, J. M., Lopez, J. M., and Corredor, J. E.: Analysis of the optical properties of the Orinoco River plume by absorption and fluorescence spectroscopy, Mar. Chem., 66, 35–51, 1999.

Del Castillo, C. E., Coble, P. G., and Müller-Karger, F. E.: On the dispersal of riverine colored dissolved organic matter over the West Florida Shelf, Limnol. Oceanogr., 45, 1452–1432, 2000.

Determann, S., Reuter, R., Wagner, P., and Willkomm, R.: Fluorescence matter in the eastern Atlantic Ocean: part 1. Method of measurement and near-surface distribution, Deep-Sea Res., 41, 659–675, 1994.

Determann, S., Reuter, R., and Willkomm, R.: Fluorescent matter in the eastern Atlantic Ocean: part 2. Vertical profiles and relation to water masses, Deep-Sea Res., 43, 345–360, 1996.

Determann, S., Lobbes, J. M., Reuter, R., and Rullkötter, J.: Ultraviolet fluorescence excitation and emission spectroscopy of marine algae and bacteria, Mar. Chem., 62, 137–156, 1998.

Devenon, J. L., Broche, P., De Maistre, J. C., Forget, P., Gagelli, J., and Rougier, G.: VHF radar measurements in the Rhone river plume, Water Pol. R., 28, 75–87, 1992.

Doval, M. D., Pérez, F. F., and Berdalet, E.: Dissolved and particulate organic carbon and nitrogen in the northwestern Mediterranean, Deep-Sea Res. Pt. I, 46, 511–527, 1999.

Durrieu de Madron, X., Denis, L., Diaz, F., Garcia, N., Guieu, C., Grenz, C., Loyë-Pilot, M. D., Ludwig, W., Moutin, T., Raimbault, P., and Ridame, C.: Nutrients and carbon budgets for the Gulf of Lion during the Moogli cruises, Oceanol. Acta, 26, 421–433, 2003.

Estournel, C., Broche, P., Marsaleix, P., Devenon, J. L., Auclair, F., and Vehil, R.: The Rhone River plume in unsteady conditions: numerical and experimental results, Estuar. Coast. Shelf S., 53, 25–38, 2001.

Ferrari, G. M.: The relationship between chromophoric dissolved organic matter and dissolved organic carbon in the European Atlantic coastal area and in the West Mediterranean Sea (Gulf of Lions), Mar. Chem., 70, 339–357, 2000.

Fontana, C., Grenz, C., Pinazo, C., Marsaleix, P., and Diaz, F.: Assimilation of SeaWiFS chlorophyll data into a 3D-coupled physical-biogeochemical model applied to a freshwater-influenced coastal zone, Cont. Shelf Res., 29, 1397–1409, 2009.

Fontana, C., Grenz, C., Pinazo, C., Marsaleix, P., and Diaz, F.: Sequential assimilation of a year-long time-series of SeaWiFS chlorophyll data into a 3D biogeochemical model on the French Mediterranean coast, Cont. Shelf Res., 30, 1761–1771, 2010.

Forget, P., Devenon, J. L., De Maistre, J. C., Broche, P., and Leveau, M.: VHF remote sensing for mapping river plume circulation, Geophys. Res. Lett., 17, 1097–1100, 1990.

Gatti, J., Petrenko, A., Devenon, J. L., Leredde, Y., and Ulses, C.: The Rhone river dilution zone present in the northeastern shelf of the Gulf of Lion in December 2003, Cont. Shelf Res., 26, 1794–1805, 2006.

Gohin, F., Druon, J. N., and Lampert, L.: A five channel chlorophyll concentration algorithm applied to SeaWiFS data processed by SeaDAS in coastal waters, Int. J. Remote Sens., 23(8), 1639–1661, 2002.

Gohin, F., Loyer, S., Lunven, M., Labry, C., Froidefond, J. M., Delmas, D., Huret, M., and Herbland, A.: Satellite-derived parameters for biological modelling in coastal waters: Illustration over the eastern continental shelf of the Bay of Biscay, Remote Sens. Environ., 95(1), 29–46, 2005.

Green, S. A. and Blough, N. V.: Optical absorption and fluorescence properties of chromophoric dissolved organic matter in natural waters, Limnol. Oceanogr., 39, 1903–1916, 1994.

Grzybowski, W.: Effect of short-term irradiation on the absorbance spectra of the chromophoric organic matter dissolved in the coastal and riverine waters, Chemosphere, 40, 1313–1318, 2000.

Hedges, J. I.: Global biogeochemical cycles: Progress and problems, Mar. Chem., 39, 67–93, 1992.

Hedges, J. I.: Why Dissolved Organics Matter? in: Biogeochemistry of Marine Dissolved Organic Matter, edited by: Hansell, D. A. and Carlson, C. A., Academic Press, San Diego, 1–27, 2002.

Helms, J. R., Stubbins, A., Ritchie, J. D., Minor, E. C., Kieber, D. J., and Mopper, K.: Absorption spectral slopes and slope ratios as indicators of molecular weight, source, and photobleaching of chromophoric dissolved organic matter, Limnol. Oceanogr., 53, 955–969, 2008.

Højerslev, N. K., Holt, N., and Aarup, T.: Optical measurements in the North Sea-Baltic Sea transition zone. I. On the origin of the deep water in the Kattegat, Cont. Shelf Res., 16(10), 1329–1342, 1996.

Huguet, A., Vacher, L., Relexans, S., Saubusse, S., Froidefond, J. M., and Parlanti, E.: Properties of fluorescent dissolved organic matter in the Gironde Estuary, Org. Geochem., 40, 706–719, 2009.

Jerlov, N. G.: Optical Oceanography, American Elsevier Publ. Co., Inc., New York, 194 pp., 1968.

Joux, F., Jeffrey, W. H., Abboudi, M., Neveux, J., Pujo-Pay, M., Oriol, L., and Naudin, J. J.: Ultraviolet Radiation in the Rhône River Lenses of Low-Salinity and in Marine Waters of the Northwestern Mediterranean Sea: Attenuation and Effects on Bacterial Activities and Net Community Production, Photochem. Photobiol., 85, 783–793, 2009.

Jumars, P. A., Penry, D. L., Baross, J. A., Perry, M. J., and Frost, B. W.: Closing the microbial loop: dissolved carbon pathway to heterotrophic bacteria from incomplete ingestion, digestion and absorption in animals, Deep-Sea Res., 36, 483–495, 1989.

Kirk, J. T. O.: Light and Photosynthesis in Aquatic Ecosystems, Second edn., Cambridge University Press, Cambridge, 410 pp., 1994.

Komada, T., Shofield, O. M. E., and Reimers, C. E.: Fluorescence characteristics of organic matter released from coastal sediments during resuspension, Mar. Chem., 79, 81–97, 2002.

Kowalczuk, P., Cooper, W. J., Whithead, R. F., Durako, M. J., and Sheldon, W.: Characterization of CDOM in an organic rich river and surrounding coastal ocean in the South Atlantic Bight, Aquat. Sci., 65, 381–398, 2003.

Lakowicz, J. R.: Principles of fluorescence spectroscopy, 3rd edn., Springer Science; New York, 158–204, 2006.

Lemée, R., Rochelle-Newall, E., Van Wambeke, F., Pizay, M. D.,

Rinaldi, P., and Gatusso, J. P.: Seasonal variation of bacterial production, respiration and growth efficiency in the open NW Mediterranean Sea, Aquat. Microb. Ecol., 29, 227–237, 2002.

Mague, T. H., Friberg, E., Hughes, D. J., and Morris, I.: Extracellular release of carbon by marine phytoplankton: A physiological approach, Limnol. Oceanogr., 25, 262–279, 1980.

Margat, J. (Ed.): L'eau dans le bassin méditerranéen, situation et prospective, in: les fascicules du Plan Bleu, vol. 6, Economica, Paris, 196 pp., 1992.

Mayer, L. M., Schick, L. L., and Loder III, T. C.: Dissolved protein fluorescence in two Maine estuaries, Mar. Chem., 64, 171–179, 1999.

Milliman, J. D., Rutkowski, C., and Meybeck, M.: River discharge to the sea: a global river index (GLORI), LOICZ Reports and Studies, LOICZ Core Project Office, Texel, Netherland Institute for Sea Research (NIOZ), 125 pp., 1995.

Mopper, K. and Kieber, D. J.: Marine photochemistry and its impact on carbon cycling, in: The effects of UV radiation in the marine environment, edited by: de Mora, S., Demers, S., and Vernet, M., Cambridge University Press, Cambridge, 101–129, 2000.

Mopper, K. and Kieber, D. J.: Photochemistry and the cycling of carbon, sulphur, nitrogen and phosphorus, in: Biogeochemistry of Marine Dissolved Organic Matter, edited by: Hansell, D. A. and Carlson, C. A., Academic Press, San Diego, 455–507, 2002.

Mopper, K. and Schultz, C. A.: Fluorescence as a possible tool for studying the nature and water column distribution of DOC components, Mar. Chem., 41, 229–238, 1993.

Moran, M. A., Sheldon Jr., W. M, and Zepp, R. G.: Carbon loss and optical property change during long term photochemical and biological degradation of estuarine dissolved organic matter, Limnol. Oceanogr., 45(6), 1254–1264, 2000.

Mueller, J. L. and Austin, R. W.: Ocean Optics Protocols for SeaWiFS Validation, Revision 1. NASA Tech. Memo. 104566, Vol. 25, edited by: Hooker, S. B., Firestone, E. R., and Acker, J. G., NASA GSFC, Greenbelt, Maryland, 67 pp., 1995.

Myklestad, S. M.: Dissolved organic carbon from phytoplankton, in: The Handbook of Environmental Chemistry, Vol. 5, Part D, edited by: Wangersky, P., Mar. Chem., Springer-Verlag Berlin/Heidelberg, Heidelberg, 111–148, 2000.

Nagata, T.: Production mechanisms of Dissolved Organic Matter, in: Microbial Ecology of the Oceans, edited by: Kirchman, D. L., 5, 121–152, 2000.

Nelson, J. R. and Guarda, S.: Particulate and dissolved spectral absorption on the continental shelf of the southeastern United States, J. Geophys. Res., 100, 8715–8732, 1995.

Nelson, N. B. and Siegel, D. A.: Chromophoric DOM in the Open Ocean, in: Biogeochemistry of Marine Dissolved Organic Matter, edited by: Hansell, D. A. and Carlson, C. A., Academic Press, San Diego, 547–578, 2002.

Nelson, N. B., Carlson, C. A., and Steinberg, D. K.: Production of chromophoric dissolved organic matter by Sargasso Sea microbes, Mar. Chem., 89, 273–287, 2004.

Nelson, N. B., Siegel, D. A., Carlson, C. A., Swan, C., Smethie Jr., W. M., and Khatiwala, S.: Hydrography of chromophoric dissolved organic matter in the North Atlantic, Deep-Sea Res. Pt. I., 54, 710–731, 2007.

Nieke, B., Reuter, R., Heuermann, R., Wang, H., Babin, M., and Therriault, J. C.: Light absorption and fluorescence properties of chromophoric dissolved organic matter (CDOM) in the St. Lawrence Estuary (Case 2 waters), Cont. Shelf Res., 17, 235–252, 1997.

Nieto-Cid, M., Alvarez-Salgado, X. A., and Perez, F.: Microbial and photochemical reactivity of fluorescent dissolved organic matter in a coastal upwelling system, Limnol. Oceanogr., 51, 1391–1400, 2006.

Ohno, T.: Fluorescence Inner-Filtering Correction for Determining the Humification Index of Dissolved Organic matter, Environ. Sci. Technol, 36, 742–746, 2002.

Opsahl, S. and Benner, R.: Distribution and cycling of terrigenous dissolved organic matter in the ocean, Nature, 386, 480–482, 1997.

Parlenti, E., Wörz, K., Geoffroy, L., and Lamotte, M.: Dissolved organic matter fluorescence spectroscopy as a tool to estimate biological activity in a coastal zone submitted to anthropogenic inputs, Org. Geochem., 31(12), 1765–1781, 2000.

Pujo-Pay, M., Conan, P., Joux, F., Oriol, L., Naudin, J. J., and Cauwet, G.: Impact of phytoplankton and bacterial production on nutrient and DOM uptake in the Rhône River plume (NW Mediterranean), Mar. Ecol-Prog. Ser., 315, 43–54, 2006.

Reffray, G., Fraunié, P., and Marsaleix, P.: Secondary flows induced by wind forcing in the Rhône region of freshwater influence, Ocean Dynam., 54, 179–196, 2004.

Romera-Castillo, C., Sarmento, H., Alvarez-Salgado, X. A., Gasol, J. M., and Marrasé, C.: Production of chromophoric dissolved organic matter by marine phytoplankton, Limnol. Oceanogr., 55, 446–454, 2010.

Ruiz, S., Gomis, D., Sotillo, M. G., and Josey, S. A.: Characterization of surface heat fuxes in the Mediterranean Sea from a 44-year high-resolution atmospheric data set, Global Planet. Change, 63, 258–274, 2008.

Santinelli, C., Gasparini, G. P., Nannicini, L., and Seritti, A.: Vertical distribution of dissolved organic carbon (DOC) in the Western Mediterranean Sea, Deep-Sea Res. Pt. I, 49, 2203–2219, 2002.

Seckmeyer, G., Pissulla, D., Glandorf, M., Henriques, D., Johnsen, B., Webb, A., Siani, A. M., Bais, A., Kjeldstad, B., Brogniez, C., Lenoble, J., Gardiner, B., Kirsch, P., Koskela, T., Kaurola, J., Uhlmann, B., Slaper, H., den Outer, P., Janouch, M., Werle, P., Gröbner, J., Mayer, B., de la Casiniere, A., Simic, S., and Carvalho, F.: Variability of UV Irradiance in Europe, Photochem. Photobiol, 84, 172–179, 2008.

Sempéré, R., Charrière, B., Cauwet, G., and Van-Wambeke, F.: Carbon inputs of the Rhône River to the Mediterranean Sea: Biogeochemical implications, Global Biogeochem. Cy., 14(2), 669–681, 2000.

Sempéré, R., Panagiotopoulos, C., Lafont, R., Marroni, B., and Van Wambeke, F.: Total organic carbon dynamics in the Aegean Sea, J. Marine Syst., 33–34, 355–364, 2002.

Seritti, A., Russo, D., Nannicini, L., and Del Vecchio, R.: DOC, absorption and fluorescence properties of estuarine and coastal waters of the northern Tyrrhenian Sea, Chem. Spec. Bioavailab., 10, 95–105, 1998.

Seritti, A., Manca, B. B., Santinelli, C., Murru, E., Boldrin, A., and Nannicini, L.: Relationships between hydrological properties and dissolved organic carbon (DOC) in the Ionian Sea (winter 1999), J. Geophys. Res.-Oceans, 108, 8112, doi:10.1029/2002JC001345, 2003.

Siegel, D. A., Maritorena, S., Nelson, N. B., Hansell, D. A., and

Lorenzi-Kayser, M.: Global distribution and dynamics of colored dissolved and detrital organic materials, J. Geophys. Res., 107(C12), 3228, doi:10.1029/2001JC000965, 2002.

Sierra, M. M. D., Donard, O. F. X., and Lamotte, M.: Behaviour of dissolved fluorescent organic matter during estuarine mixing, Mar. Chem., 58, 51–58, 1997.

Sierra, M. M. D., Giovanela, M., Parlanti, E., and Soriano-Sierra, E. J.: Fluorescence fingerprint of fulvic and humic acids from varied origins as viewed by single-scan and excitation/emission matrix techniques, Chemosphere, 58, 715–733, 2005.

Sohrin, R. and Sempéré, R.: Seasonal variation in total organic carbon in the Northeast Atlantic in 2000–2001, J. Geophys. Res., 110, C10S90, doi:10.1029/2004JC002731, 2005.

Smith, S. V. and Hollibaugh, J. T.: Coastal metabolism and the oceanic organic carbon balance, Rev. Geophys., 31, 75–89, 1993.

Stedmon, C. A. and Markager, S.: Tracing the production and degradation of autochthonous fractions of dissolved organic matter using fluorescence analysis, Limnol. Oceanogr., 50, 1415–1426, 2005.

Stedmon, C. A., Markager, S., and Kaas, H.: Optical properties and signatures of chromophoric dissolved organic matter (CDOM) in Danish coastal waters, Estuar. Coast. Shelf S., 51, 267–278, 2000.

Tedetti, M. and Sempéré, R.: Penetration of UV radiation in the marine environment: A review, Photochem. Photobiol., 82, 389–397, 2006.

Tedetti, M., Guigue, C., and Goutx, M.: Utilization of a submersible UV fluorometer for monitoring anthropogenic inputs in the Mediterranean coastal waters, Mar. Pollut. Bull., 60, 350–362, 2010.

The MERMEX Group: Marine Ecosystems Responses to climatic and anthropogenic forcings in the Mediterranean, Prog. Oceanogr., in review, 2010.

Vähätalo, A. V. and Wetzel, R. G.: Photochemical and microbial decomposition of chromophoric dissolved organic matter during long (months-years) exposures, Mar. Chem., 89, 313–326, 2004.

Vasilkov, A., Krotkov, N., Herman, J., Mc Clain, C., Arrigo, K., and Robinson, W.: Global mapping of underwater UV irradiances and DNA-weighted exposures using Total Ozone Mapping Spectrometer and Sea-viewing Wide Field-of-view Sensor data products, J. Geophys. Res., 106, 27205–27219, 2001.

Vignudelli, S., Santinelli, C., Murru, E., Nannicini, L., and Seritti, A.: Distributions of dissolved organic carbon (DOC) and chromophoric dissolved organic matter (CDOM) in coastal waters of the northern Tyrrhenian Sea (Italy), Estuar. Coast. Shelf S., 60, 133–149, 2004.

Vodacek, A., Blough, N. V., DeGrandpre, M. D., Peltzer, E. T., and Nelson, R. K.: Seasonal variation of CDOM and DOC in the Middle Atlantic Bight: terrestrial inputs and photooxidation, Limnol. Oceanogr., 42(2), 674–686, 1997.

Yamashita, Y. and Tanoue, E.: Chemical characterization of protein-like fluorophores in DOM in relation to aromatic amino acids, Mar. Chem., 82, 255–271, 2003.

Zsolnay, A., Baigar, E., Jimenez, M., Steinweg, B., and Saccomandi, F.: Differentiating with fluorescence spectroscopy the sources of dissolved organic matter in soils subjected to drying, Chemosphere, 38, 45–50, 1999.